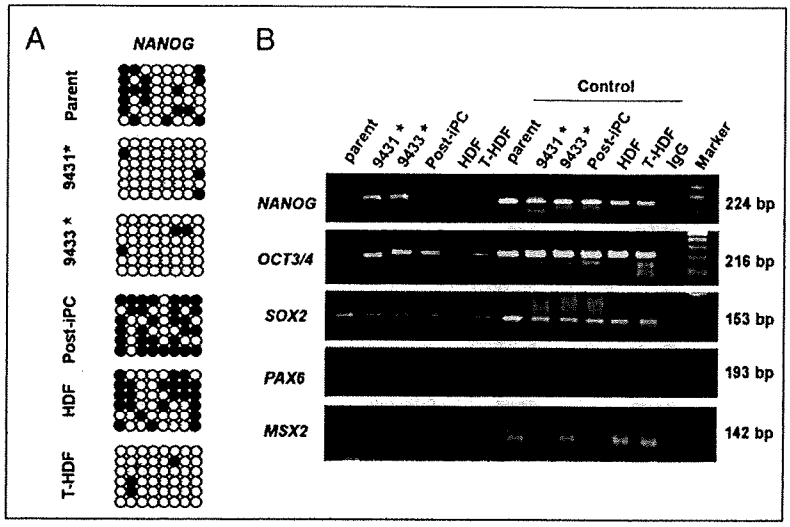

Fig. 4. Epigenetic modification of immature status-related genes evaluated with bisulfite sequencing analysis and chromatin immunoprecipitation in DLD-1. (*A*) From the analysis of epigenetic status, bisulfite genomic sequencing analyses in the promoter regions of genes inducing immature status, *NANOG*, revealed that they were not methylated appreciably in iPC cells (clones 9431 and 9433), whereas the CpG dinucleotides of the regions were methylated in parental cancer cells and PostiPC cells (open and closed circles indicate unmethylated and methylated, respectively). (*B*) Chromatin immunoprecipitation with trimethyl-K4 H3 antibody was used to analyze the histone modification status in parental, iPC, and PostiPC cells. H3 lysine 4 was methylated in these regions for *NANOG* in iPC cells compared to that in parental and PostiPC cells. H3 lysine 4 was methylated in these regions for *OCT3/4* in iPC and PostiPC cells compared to those in parental cells (results were assessed in contrast to each input DNA). HDF and transfected HDF (T-HDF) were analyzed for comparison. As a control, respective sheared chromatin sample was used for quantitative PCR. *, clones of iPC cells.

Assessment of Tumorigenic Properties. To determine tumorigenic properties in vivo, PostiPC cells were transplanted s.c. at several densities into dorsal flanks of NOD/SCID mice. Four weeks after injection, we observed tumor formation (Fig. S3*A*). There were significant differences between PostiPC cells and parental cells ($P < 0.01$, Wilcoxon rank test; Fig. S3*B*). These data demonstrated the reduction of tumorigenesis via reprogramming process; this finding may be applied to anticancer therapy.

Discussion

The role of CSCs was noted in acute myeloid leukemia (3). The possible involvement of CSCs has since been shown in several solid tumors (20–22). In solid tumors, these results suggest that the CSC population, although it is likely a minority, is related to treatment resistance and problems of relapse or metastasis (1, 2). CSCs, through their self-renewal and drug-resistant capacities, may share properties that are conducive to persistence and proliferation, even after anticancer therapy. It is important to understand their biological characteristics, as specific markers of all CSCs have not yet been identified.

Recently, several reports have shown that tumor development is associated with genetic and epigenetic changes of the genome, and that epigenetic modifications play an important role in tumor heterogeneity (23). Several experiments, such as nuclear transplantation, ES cell fusion, and transfection with several transcription factors, have demonstrated reprogramming of terminally differentiated cells into pluripotent embryonic cells, which is linked to the development of an organism by resetting the epigenetic modifications (4–9). In previous reports, the transcription factor *NANOG* was required to maintain the pluripotency and self-renewal of ES cells (13, 14).

According to genetic and epigenetic analyses in previous reports, immature status related to promoter activation in defined genes, such as *NANOG*, plays a very important role in the establishment of a pluripotent state (6–9, 13, 14). To prepare iPC cells, we manufactured a specific tool that could detect the pluripotent

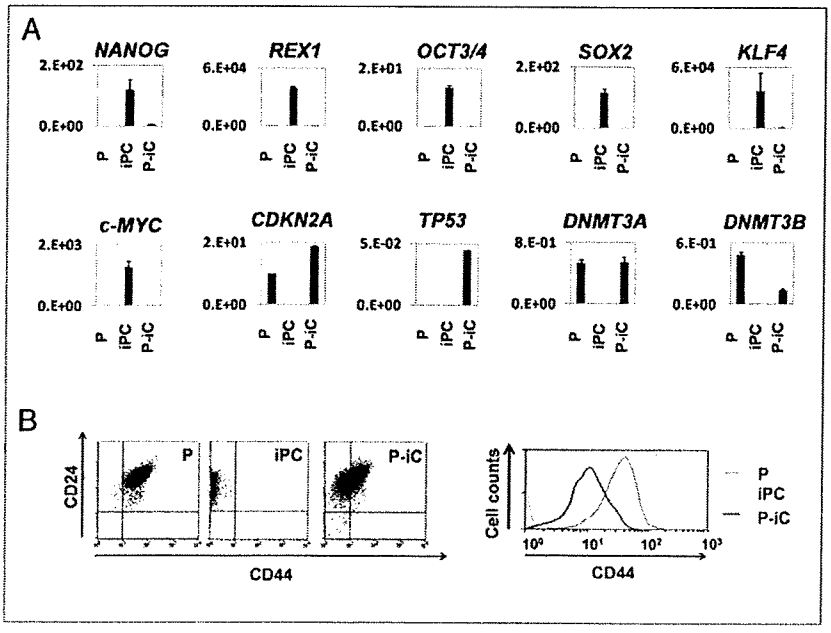

Fig. 5. Expression of immature and differentiated status-related genes in parental, iPC, and PostiPC cells induced from DLD-1. (*A*) The expression of *NANOG, REX1, OCT3/4, SOX2, KLF4, and c-MYC* markedly decreased in iPC cells. The expression of *CDKN2A, DNMT3A,* and *DNMT3B* increased in PostiPC cells compared to iPC cells. The mRNA copy expression was normalized against *GAPDH* mRNA expression. (*B*) (*Left*) Flow cytometry showed a shift of the CD24/CD44 population in parental, iPC, and PostiPC cells. (*Right*) The CD44 population in PostiPC cells decreased compared with that of parental cells. P, parental cells; P-iC, PostiPC cells.

CELL BIOLOGY

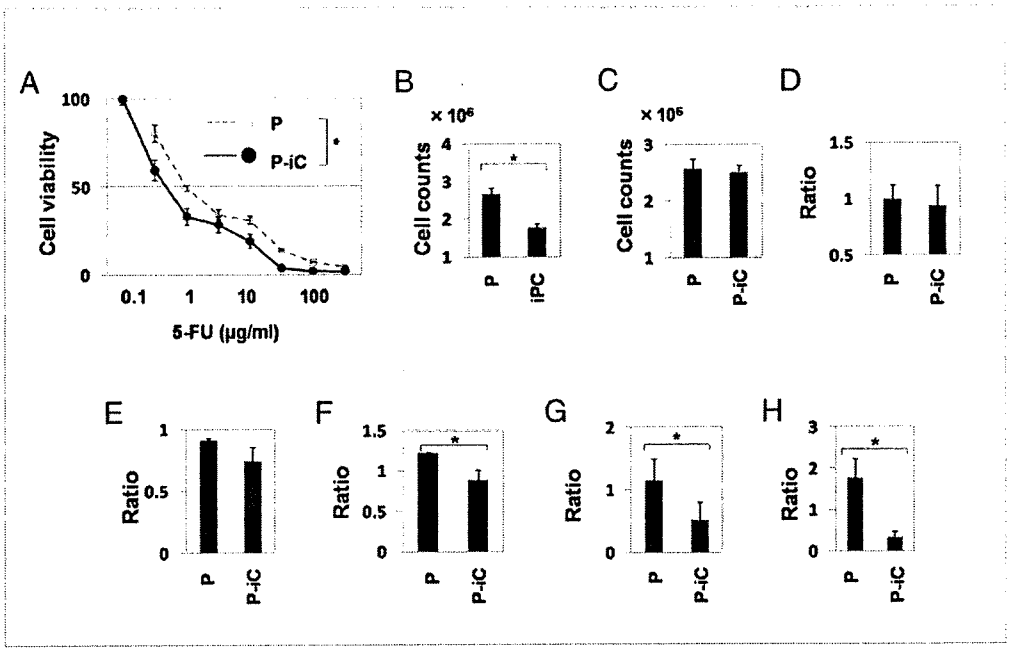

Fig. 6. In vitro methyl thiazolyl tetrazolium (MTT) analyses, proliferation and invasion assay. (*A*) The 5-FU MTT assay revealed significant differences in PostiPC and DLD-1 parental cells ($n = 11$, $P = 0.003$, Wilcoxon rank test). (*B*) Proliferation assays for ES-culture conditions showed differences in growth of iPC cells and DLD-1 parental cells ($n = 4$, $P = 0.046$, Wilcoxon rank test). (*C*) Proliferation assays in primary culture conditions showed no significant differences between DLD-1 parental and PostiPC cells. (*D*) Invasion assay showed no significant differences between DLD-1 parental and PostiPC cells (relative ratio and parental cell average). (*E* and *F*) Proliferation assays showed differences in ratio with control (with no treatment) under the differentiation-inducing treatment with vitamins A and D supplementation ($n = 8$, $P = 0.512$ and 0.049, respectively, Wilcoxon rank test). (*G* and *H*) Invasion assays showed significant differences in the ratio with control (with no treatment) cells under the differentiation-inducing treatment with vitamin A and D supplementation ($n = 6$, $P = 0.013$ and 0.003, respectively, Wilcoxon rank test). P, parental cells; P-iC, PostiPC cells. *, $P < 0.05$.

state in living cells based on the results of previous studies. We investigated *NANOG* expression in gastrointestinal cancer cell lines, corresponding to human iPS cells and teratocarcinoma NTERA-2, which had higher *NANOG* expression. The expression could not be detected in PostiPC cells with this system. A low efficiency, as shown in iPS (6–9, 13, 14), suggests a possibility that only a minority of tumor cell lines possesses specific potential to obtain the property of iPC, or more likely that multiple mechanisms are involved in full execution of reprogramming. We have to consider a possibility that sphere-forming cells might be rare among the original cancer cell populations.

In this study, the tumor-suppressor gene *P16(INK4A)*, which acts against the self-renewal of ES cells (10, 12), was repressed in iPC cells. Our analysis indicated that *P16(INK4A)* expression increased in PostiPC cells, which may relate to the notion that *P16(INK4A)* up-regulation is involved in the suppression of transformed phenotypes and their sensitization to therapeutic agents (24). The sequence study of *P16(INK4A)* promoter indicated the demethylation in PostiPC cells from DLD-1 cells, whereas the sequence of parental cells was methylated. This study suggests that the reactivation of tumor suppressor genes by reprogramming may play a role in increased chemosensitivity to 5-FU and the regression of cell proliferation and invasiveness under differentiation-inducing conditions. The *Rb/P16(INK4A)* tumor-suppressive pathway has been reported to be abrogated in several tumors (24). It is necessary to investigate the specific analysis in the pathways to assess the contribution of TSG.

Presumably, the suppression of tumors and their sensitization to induced differentiation are the result of genetic and epigenetic modifications. This result supports the possibility of new cancer therapies via reprogramming approaches even in cancer cells that should have corrupted genetic codes. In the present study, iPC cells were induced from eight cancer cells, including cancers of colorectum, esophagus, stomach, pancreas, liver and bile ducts (Fig. S4). Here, iPC was established from cancer cell lines. It is necessary to demonstrate universality in primary tumors and to more efficiently investigate the factors and population in relation to the induction of iPC cells: points to be elucidated and developed include differences of normal and tumor cells, individual responses, efficiency, and reagent delivery system. As novel therapeutic approaches, the heterogeneity of reprogrammed cancer cells remains to be investigated.

Materials and Methods

Cell Lines and Culture. Twenty cell lines derived from human gastrointestinal cancers included colorectal cancer (Caco2, DLD-1, HCT116, HT-29, KM12SM, LoVo, and SW480), esophageal cancer (TE-10), gastric cancer (MKN45), pancreatic cancer (BXPC-3, MIAPaCa-2, PANC-1, and PSN-1), hepatocellular carcinoma (Hep3B, HepG2, HLE, HLF, HuH-7, and PLC), cholangiocellular carcinoma (HuCCT-1), and teratocarcinoma (NTERA-2 clone D1). NTERA-2 was provided by DS Pharma Biomedical (Osaka). These cell lines were maintained in DMEM (Nakalai Tesque, Kyoto) containing 10% FBS at 37 °C under a 5% humidified CO_2 atmosphere. HDF was purchased from Toyobo (CA106K05a; Osaka) as a normal cell control and maintained with the Fibroblast Growth Medium kit (CA116500; Toyobo). Plasmids were purchased from Addgene (Cambridge, MA), Clontech (Palo Alto, CA), Cell Biolabs (San Diego), and Open Biosystems (Huntsville, AL). The plasmids used in this study are summarized in Table S1. These transfectants were grown in DMEM supplemented with 10% FBS and puromycin (2 μg/mL), and transferred to specific culture conditions as described in the supporting information. All transfectants with retrovirus were made with the ViraDuctin retrovirus transduction kit (Cell Biolabs). Those with lentivirus were made with the Virapower packaging mix (Invitrogen, Carlsbad, CA) or Arrest-In (Open Biosystems). In brief, cancer cell lines were transfected with adequate plasmid at a concentration of 4 μg/μl by using lipofectamine (Lipofectamine 2000; Invitrogen), and incubated in glucose-free Opti-MEM (Invitrogen). All experiments were performed at 50–70% cell confluence and results were confirmed in at least three independent experiments. All-in-one-type fluorescence microscopy

(BZ-8000; Keyence, Osaka) with digital photographic capability was used to visualize cells at several magnifications. The growth rates of the cultured gastrointestinal cancer cell lines were measured by counting cells using Cell-Tac (Nihon Koden, Tokyo). The optimization of retroviral transduction of human cancer cell lines was performed as shown in supporting information. Vectors used are shown in Table S1.

RNA Preparation and RT-PCR. Total RNA was prepared by using TRIzol reagent (Invitrogen). Reverse transcription was performed with SuperScriptIII (Invitrogen). To confirm PCR amplification, 25–35 cycles of the PCR were performed by using a PCR kit (Takara, Kyoto) on a Geneamp PCR system 9600 (PE Applied Biosystems, Foster City, CA) with the following condition: 95 °C for 10 s, 60 °C for 10 s, and 72 °C for 60 s. An 8-μl aliquot of each reaction mixture was size-fractionated in a 1.5% agarose gel and visualized with ethidium bromide staining. To confirm RNA quality, PCR amplification was performed for the glyceraldehyde-3-phosphate dehydrogenase (*GAPDH*) gene using the specific primers (Tables S2 and S3). For quantitative assessment, we evaluated the gene expression by RT-PCR analysis. Quantitative real-time RT-PCR was performed by using a LightCycler TaqMan Master kit (Roche Diagnostics, Tokyo) for cDNA amplification of target specific genes. The expression of mRNA copies was normalized against *GAPDH* mRNA expression. The detailed condition for Quantitative real-time RT-PCR assessment is shown in supporting information. Primers used are shown in Tables S2 and S3.

Drugs and Antibodies. Antibodies used for immunocytology were against Nanog, Ssea-3, Ssea-4, Tra-1-60, Tra-1-81, Tra-2-49, Tubb3, Gfap, Vim (Chemicon International, Temecula, CA), and Krt19 (OriGene Technologies, Rockville, MD). Differentiation to adipocytes was induced by specific supplements (Adipogenic Supplement 390416; Invitrogen).

Bisulfite Sequencing. Genomic DNA was treated with Applied Biosystems methySEQr Bisulfite Conversion kit (Applied Biosystems) according to the manufacturer's recommendations. Treated DNA was purified with QIAquick column (Qiagen, Valencia, CA). The human *NANOG* gene promoter regions were amplified by PCR. The PCR products were subcloned with pCR2.1-TOPO. Every clone of each sample was verified by sequencing with the T3 and T7 primers. The analysis used Sequencing Analysis Software v5.2 (Applied Biosystems). Primer sequences used for PCR amplification are provided in Table S3.

Chromatin Immunoprecipitation Assay. Approximately 1×10^7 cells were cross-linked with 1% formaldehyde for 10 min at room temperature and quenched by adding glycine. The cell lysate was treated to share a chromatin-DNA complex with an enzymatic shearing kit (Active Motif, Carlsbad, CA). Immunoprecipitation used Protein G magnetic beads (Active Motif)-linked anti-trimethyl lysine 4 histone H3 antibody (Nippongene, Toyama, Japan), or a negative control IgG kit (Active Motif). Eluates were used as templates for quantitative PCR. Each sheared chromatin sample was used for quantitative PCR as a control. Primer sequences used for PCR amplification are provided in Table S3.

Flow Cytometry. Flow cytometry was performed on trypsin-dissociated parental cells, iPC, and PostiPC cells by using antibodies for CD24 (BD Biosciences, Sparks, MD) and CD44 (BD Biosciences). 7-AAD (eBioscience, San Diego, CA) preincubation was used to exclude dead cells. To assess the expression of the reprogrammed cells, iPC cells were assessed in the isolated colonies after the transfection of *NANOG* promoter-*GFP* clone. Cells were analyzed by using a FACScan flow cytometer equipped with CellQuest software (FACS caliber; BD Biosciences).

RA and VD3 Treatment. RA and VD3 were purchased from Sigma–Aldrich (St. Louis). RA was dissolved in 99% ethanol as a 100 μM stock solution. The cells were allowed to settle for 48 h in DMEM supplemented with 100 nM RA. VD3 was dissolved in 99% ethanol as a 10 M stock solution. The cells were allowed to settle for 48 h in DMEM supplemented with 10 nM VD3. To assess the proliferation in the presence of RA and VD3, the cells were grown in these media for another 48 h. Cell viability was determined with the Cell Counting kit incorporating WST-8 (Dojindo Lab., Tokyo). WST-8 (10 μL) was added to 100 μL of the medium containing each supplement above, and the absorbance was read at 450 nm by using a microplate reader (Model 680XR; Bio-Rad Laboratories, Hercules). All experiments were performed at 30–80% cell confluence, and the results were confirmed in at least three independent experiments.

Chemosensitivity Assessment. To assess the sensitivity to 5-FU in vitro, cells at different concentrations were evaluated with an MTT assay. 5-FU was purchased from Kyowa Hakkou (Tokyo). The cells were allowed to settle for 96 h in DMEM supplemented with several concentrations of 5-FU, and viability was assessed.

Invasion Assays. Cell invasion was assessed with a CytoSelect Cell Invasion Assay according to the manufacturer's protocol (Cell Biolabs). Cells (1.0×10^5) in DMEM were placed on 8.0-m-pore size membrane inserts in 96-well plates, and DMEM with 10% FBS was placed in the bottom of the wells. After 24 h, cells that did not invade were removed from the top side of the membrane chamber, and the cells from the underside of the membrane were completely dislodged by tilting the membrane chamber in Cell Detachment Solution (Cell Biolabs). Lysis Buffer/CyQuannt GR dye solution (Cell Biolabs) was added to each well, and the fluorescence of the mixture was read with a fluorescence plate reader at 480 nm/520 nm.

In Vivo Analysis. The tumorigenic properties were evaluated on trypsin-dissociated cells with parental and PostiPC cells. We transplanted them suspended in DMEM/Matrigel (BD Biosciences) s.c. into the dorsal flanks of NOD/SCID mice (CREA, Tokyo) in several concentrations. Tumors were dissected and measured 4 weeks after injection.

Statistical Analysis. For continuous variables, the results are expressed as means ± SEs of the mean. The relationships among gene expressions or cell counts were analyzed with χ^2 and Wilcoxon rank tests. All tests were analyzed with JMP software (SAS Institute, Cary, NC). Differences with P values <0.05 were considered statistically significant.

1. Reya T, Morrison SJ, Clarke MF, Weissman IL (2001) Stem cells, cancer, and cancer stem cells. *Nature* 414:105–111.
2. Pardal R, Clarke MF, Morrison SJ (2003) Applying the principles of stem-cell biology to cancer. *Nat Rev Cancer* 3:895–902.
3. Bonnet D, Dick JE (1997) Human acute myeloid leukemia is organized as a hierarchy that originates from a primitive hematopoietic cell. *Nat Med* 3:730–737.
4. Thomson JA, et al. (1998) Embryonic stem cell lines derived from human blastocysts. *Science* 282:1145–1147.
5. Hochedlinger K, Jaenisch R (2006) Nuclear reprogramming and pluripotency. *Nature* 441:1061–1067.
6. Takahashi K, Yamanaka S (2006) Induction of pluripotent stem cells from mouse embryonic and adult fibroblast cultures by defined factors. *Cell* 126:663–676.
7. Takahashi K, et al. (2007) Induction of pluripotent stem cells from adult human fibroblasts by defined factors. *Cell* 131:861–872.
8. Yu J, et al. (2007) Induced pluripotent stem cell lines derived from human somatic cells. *Science* 318:1917–1920.
9. Yu J, et al. (2009) Human induced pluripotent stem cells free of vector and transgene sequences. *Science* 324:797–801.
10. Dabelsteen S, et al. (2009) Epithelial cells derived from human embryonic stem cells display p16INK4A senescence, hypermotility, and differentiation properties shared by many P63+ somatic cell types. *Stem Cells* 27:1388–1399.
11. Hong H, et al. (2009) Suppression of induced pluripotent stem cell generation by the p53-p21 pathway. *Nature* 460:1132–1135.
12. Li H, et al. (2009) The Ink4/Arf locus is a barrier for iPS cell reprogramming. *Nature* 460:1136–1139.
13. Loh YH, et al. (2006) The Oct4 and Nanog transcription network regulates pluripotency in mouse embryonic stem cells. *Nat Genet* 38:431–440.
14. Wu Q, et al. (2006) Sall4 interacts with Nanog and co-occupies Nanog genomic sites in embryonic stem cells. *J Biol Chem* 281:24090–24094.
15. Adewumi O, et al.;International Stem Cell Initiative (2007) Characterization of human embryonic stem cell lines by the International Stem Cell Initiative. *Nat Biotechnol* 25: 803–816.
16. Vermeulen L, et al. (2008) Single-cell cloning of colon cancer stem cells reveals a multi-lineage differentiation capacity. *Proc Natl Acad Sci USA* 105:13427–13432.
17. Du L, et al. (2008) CD44 is of functional importance for colorectal cancer stem cells. *Clin Cancer Res* 14:6751–6760.
18. Huang ME, et al. (1988) Use of all-trans retinoic acid in the treatment of acute promyelocytic leukemia. *Blood* 72:567–572.
19. zur Nieden NI, Kempka G, Ahr HJ (2003) In vitro differentiation of embryonic stem cells into mineralized osteoblasts. *Differentiation* 71:18–27.
20. Singh SK, et al. (2004) Identification of human brain tumour initiating cells. *Nature* 432:396–401.
21. Kim CF, et al. (2005) Identification of bronchioalveolar stem cells in normal lung and lung cancer. *Cell* 121:823–835.
22. O'Brien CA, Pollett A, Gallinger S, Dick JE (2007) A human colon cancer cell capable of initiating tumour growth in immunodeficient mice. *Nature* 445:106–110.
23. Hahn WC, Weinberg RA (2002) Rules for making human tumor cells. *N Engl J Med* 347:1593–1603.
24. Sherr CJ, McCormick F (2002) The RB and p53 pathways in cancer. *Cancer Cell* 2: 103–112.

FEBS Letters 583 (2009) 2710–2714

ELSEVIER

FEBS Letters

journal homepage: www.FEBSLetters.org

Mdmx enhances p53 ubiquitination by altering the substrate preference of the Mdm2 ubiquitin ligase

Koji Okamoto [a,b,c], Yoichi Taya [b,c,1], Hitoshi Nakagama [a,*]

[a] National Cancer Center Research Institute, Early Oncogenesis Research Project, 5-1-1 Tsukiji, Chuo-ku, Tokyo 104-0045, Japan
[b] National Cancer Center Research Institute, Radiobiology Division, 5-1-1 Tsukiji, Chuo-ku, Tokyo 104-0045, Japan
[c] SORST, Japan Science and Technology Corporation, Japan

ARTICLE INFO

Article history:
Received 11 May 2009
Revised 26 June 2009
Accepted 13 July 2009
Available online 18 July 2009

Edited by Noboru Mizushima

Keywords:
Mdmx
Mdm2
p53
Ubiquitination

ABSTRACT

***mdm2* and *mdmx* oncogenes play essential yet non-redundant roles in synergistic inactivation of the tumor suppressor, p53. While Mdm2 inhibits p53 activity mainly by augmenting its ubiquitination, the functional role of Mdmx on p53 ubiquitination remains obscure. In transfected H1299 cells, Mdmx augmented Mdm2-mediated ubiquitination of p53. In in vitro ubiquitination assays, the Mdmx/Mdm2 heteromeric complex, in comparison to the Mdm2 homomer, showed enhanced ubiquitinase activity toward p53 and the reduced auto-ubiquitination of Mdm2. Alteration of the substrate specificity via binding to Mdmx may contribute to efficient ubiquitination and inactivation of p53 by Mdm2.**

Structured summary:
MINT-7219995: *P53* (uniprotkb:P04637) *physically interacts* (MI:0914) with *Ubiquitin* (uniprotkb:P62988) by *anti bait coimmunoprecipitation* (MI:0006)
MINT-7220023: *Ubiquitin* (uniprotkb:P62988) *physically interacts* (MI:0914) with *P53* (uniprotkb:P04637) by *pull down* (MI:0096)

1. Introduction

The p53 tumor suppressor protein plays a central role in preventing tumorigenesis. p53 functions as a sequence-specific transcriptional factor [1,2], and activated p53 exerts its function as a tumor suppressor by inducing numerous target genes [3–6]. In most cancer cells, its activity is lost via alteration of its gene or via other cellular events that inactivate p53 [7–9].

Mdm2 and Mdmx function as two major players in the suppression of p53 activity [10]. Accumulating reports indicate that the major function of Mdm2 in suppressing p53 is attributed to Mdm2-dependent p53 ubiquitination, which triggers proteasomal degradation or nuclear export of p53 [11], although it has been reported that Mdm2 inactivates p53 by other mechanisms [12–15]. Mdm2 possesses a RING finger domain, a protein–protein interaction motif that is found in many eukaryotic proteins and often possesses E3 ubiquitin ligase activity [16]. Indeed, Mdm2 functions as an E3 ubiquitin ligase, and the RING domain of Mdm2 is essential for its ubiquitin ligase activity toward p53 and Mdm2 itself [17–19].

Mdmx shares an extensive structural homology with Mdm2, and forms a heterodimer complex with Mdm2 through their RING finger domains [20,21], yet Mdmx in itself lacks the robust activity of an E3 ubiquitin ligase [22]. Thus, both genetic and biochemical evidence indicates that Mdmx and Mdm2 perform distinct yet co-operative functions in p53 inactivation.

Recent reports suggest that Mdmx may inactivate p53 by augmenting Mdm2-mediated ubiquitination of p53 [23–25]. However, precise mechanism by which Mdmx stimulates p53 ubiquitination by Mdm2 is not yet known.

In this paper, we demonstrated that wild-type Mdmx is capable of enhancing Mdm2-mediated p53 ubiquitination in vivo. Further, the in vitro study using purified Mdm2 or the Mdm2/Mdmx complex revealed that, when complexed with Mdmx, the extent of p53 ubiquitination by Mdm2 was enhanced while poly-ubiquitination of Mdm2 was significantly decreased. We propose that the effect of Mdmx on the preference of the substrate of the Mdm2 ubiquitin ligase plays an important role in effective ubiquitination of p53.

* Corresponding author.
E-mail address: hnakagam@ncc.go.jp (H. Nakagama).
[1] Present address: Cancer Science Institute of Singapore, National University of Singapore, Singapore 117456, Singapore.

0014-5793/$36.00 © 2009 Federation of European Biochemical Societies. Published by Elsevier B.V. All rights reserved.
doi:10.1016/j.febslet.2009.07.021

2. Materials and methods

2.1. DNA transfection

In DNA transfection experiments using H1299 cells, 2 μg of DNA and 4 μl of Lipofectamine 2000 reagent (Invitrogen) were introduced per 2.0×10^5 cells according to manufacturer's protocol. Cells were then incubated for 20 h before harvesting.

2.2. In vivo ubiquitination assay

For detection of p53 conjugated with endogenous ubiquitin, in vivo ubiquitination assays were performed as previously described [26] with some modifications. Transfected H1299 cells were lysed in SDS lysis buffer (50 mM Tris, pH 7.5, 100 mM NaCl, 1% SDS) supplemented with 1 mM DTT and protease inhibitor cocktail (PI) [27], boiled for 10 min, and diluted with ×4 volumes of dilution buffer (50 mM Tris, pH 7.5, 100 mM NaCl, 1.25% Triton X-100) supplemented with DTT and PI. After sonication of the lysates, p53 was immunoprecipitated with anti-p53 antibody (DO-1). Subsequently the immunoprecipitates were washed three times with 200-NP buffer [27], and analyzed by Western blotting with DO-1 and anti-ubiquitin antibody (FK2, MBL).

For detection of p53 conjugated with transfected $(His)_6$-ubiquitin, transfected H1299 cells were lysed in urea lysis buffer (100 mM NaH2PO4, 10 mM Tris–HCl, pH 8.0, 500 mM NaCl, 10% glycerol, 0.1% Triton X-100, 10 mM imidazole) supplemented with 10 mM β-mercaptoethanol, PI, 5 mM Iodoacetamide, and 1 mg/ml NEM. Proteins conjugated with His-tagged ubiquitin were purified as described before [28], and analyzed by Western blot analysis.

2.3. Protein expression and purification

Flag-tagged Human Mdm2 (Flag-Mdm2) or Human Mdmx RNA was transcribed from the corresponding cDNA using the Wheat Germ Expression Kit (Cell Free Science, Japan). Subsequently, the Flag-Mdm2 RNA alone or in combination with an excess amount of the Mdmx RNA was used for in vitro translation with wheat germ lysate (Cell Free Science) according to the manufacturer's instructions. Flag-Mdm2 or the Flag-Mdm2/Mdmx complex was then purified on agarose conjugated with anti-Flag antibody.

2.4. In vitro ubiquitination assay

In vitro ubiquitination assays were performed as previously described with some modifications [29]. Approximately 100 ng of Flag-Mdm2 or the Flag-Mdm2/Mdmx complex were mixed with the following purified components; 8 ng of GST-p53, 10 ng of E1 (Boston Biochem), 80 ng of E2 (UbcH5b, Boston Biochem), 3 μg of His-ubiquitin (Calbiochem), or methylated ubiquitin (Boston Biochem). In experiments shown in Fig. 4D, ^{125}I-ubiquitin (Perkin–Elmer) was included in the reaction mixture. These components were incubated in a reaction buffer (40 mM Tris–HCl, pH 7.5, 5 mM $MgCl_2$, 10 mM NaCl) in the presence of 2 mM Mg–ATP at 37 °C for the indicated times. After the reactions were terminated by adding SDS sample buffer, ubiquitinated proteins were separated in SDS–PAGE gels and detected by Western blot analyses or autoradiography.

3. Results

3.1. Wild-type Mdmx was capable of enhancing p53 ubiquitination in the presence of Mdm2 in vivo

Recently, we demonstrated that the non-phosphorylatable, active form of Mdmx augments p53 ubiquitination mediated by wild-type Mdm2 in transfected H1299 cells [30]. In order to determine whether wild-type Mdmx cooperates with Mdm2 to induce ubiquitination of p53 as well, wild-type Mdmx (Mdmx-wt) or the non-phosphorylated form of Mdmx (Mdmx-3A) was transfected together with Mdm2 into H1299 cells, and conjugation of p53 with endogenous ubiquitin was examined by Western blot analyses (Fig. 1). As expected from previous observation [30], Mdmx-3A, which is resistant to Mdm2-mediated ubiquitination and degradation, was expressed at higher levels than wild-type Mdmx (Fig. 1, lanes 2 and 3). p53 ubiquitination induced by Mdm2 was enhanced in the presence of co-transfected wild-type Mdmx (Fig. 1, lanes 5 and 8), indicating that wild-type Mdmx is capable of stimulating Mdm2-mediated ubiquitination of p53,

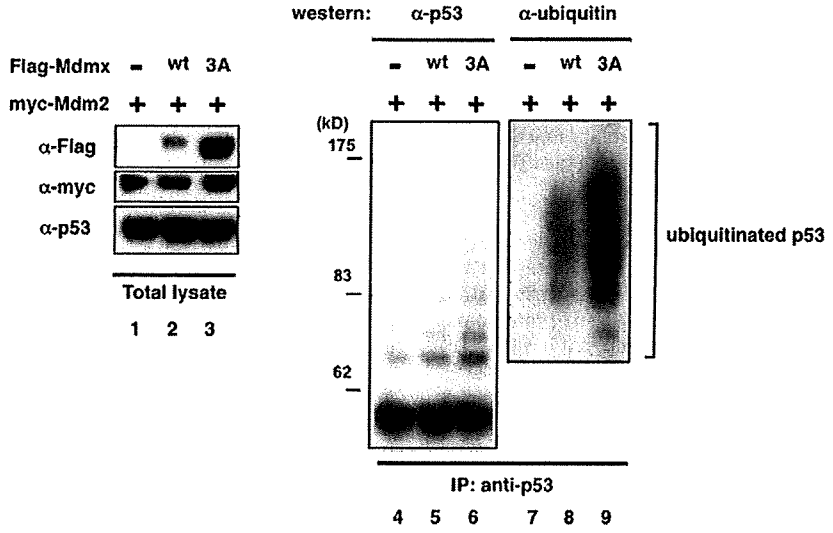

Fig. 1. Mdmx cooperates with Mdm2 to induce p53 ubiquitination. HA-p53 (0.15 mg) and either 0.4 mg of the control vector, wild-type Flag-Mdmx, or the Flag-Mdmx-3A mutant were transfected into H1299 cells in the presence of 0.2 mg of Myc-Mdm2. The total amount of transfected DNA was adjusted to 2 μg with pBluescript plasmid (Stratagene). Twenty hours after transfection, lysates prepared under denaturing conditions were used for immunoprecipitaiton with anti-p53 (DO-1) antibody. The immunoprecipitates were then used for Western blot analyses with DO-1 (left panel, and right bottom panel for low exposure) and with anti-ubiquitin antibody (right panel). Amounts of immunoprecipitates used for Western were normalized such that an equal amount of non-ubiquitinated p53 was loaded in each lane.

although the extent of the stimulation is less than that induced by the non-phosphorylatable mutant (Fig. 1, lanes 6 and 9).

3.2. Mutation at the C-terminal ubiquitinated lysines largely abolished p53 ubiquitination by Mdmx

It has been documented that Mdm2 ubiquitinates p53 at the six C-terminal lysines, the integrity of which are required for its nuclear export [31,32]. We created a mutant p53 in which all six lysines at the C-terminal domain (Fig. S1) were substituted by arginine (p53-K6R), and introduced wild-type p53 or the K6R mutant into H1299 cells together with Mdm2 in the presence or absence of Mdmx-3A. Examination of p53 ubiquitination in vivo revealed that the K6R mutation eliminates a majority of p53 ubiquitination enhanced by Mdmx (Fig. S2), indicating the six lysines were major sites for Mdmx-dependent ubiquitination.

3.3. Association of Mdmx with Mdm2 augments the ability of Mdm2 to ubiquitinate p53 and inhibits poly-ubiquitination of Mdm2 in vitro

In order to determine whether Mdmx enhances Mdm2-dependent ubiquitination of p53 via direct association with Mdm2, we next performed in vitro ubiquitination assays using purified recombinant proteins of Mdm2 or an Mdm2/Mdmx complex (see Section 2). Silver staining of the purified proteins indicated that the co-purified Mdmx formed a complex with Mdm2 at approximately a 1:1 molar ratio (Fig. 2A, right panel).

In order to determine the effect of the association with Mdmx on the activity of E3 ubiquitin ligase of Mdm2, homomeric Mdm2 or the Mdmx/Mdm2 complex was incubated with E1, E2 (UbcH5b), GST-p53, and ubiquitin, and time-course analyses of the ubiquitination of p53 and auto-ubiquitination of Mdm2 were simultaneously performed. The complex formation of Mdm2 with Mdmx-3A or with wild-type Mdmx resulted in an increase of p53 ubiquitination (Fig. 2B and C). In contrast, the Mdmx/Mdm2 complex showed a marked decrease in poly-ubiquitinated forms of Mdm2 in comparison to homomeric Mdm2 (Fig. 2B and C), indicating that the association with Mdmx-3A augments Mdm2-dependent p53 ubiquitination while it inhibits poly-ubiquitination of Mdm2.

3.4. Mdmx inhibits ubiquitination of the Mdm2-containing enzymatic complex

In order to confirm that Mdmx inhibits auto-ubiquitination of Mdm2, in vitro ubiquitination assays of the Mdm2 homomer or the Mdm2/Mdmx complex were performed in the presence of

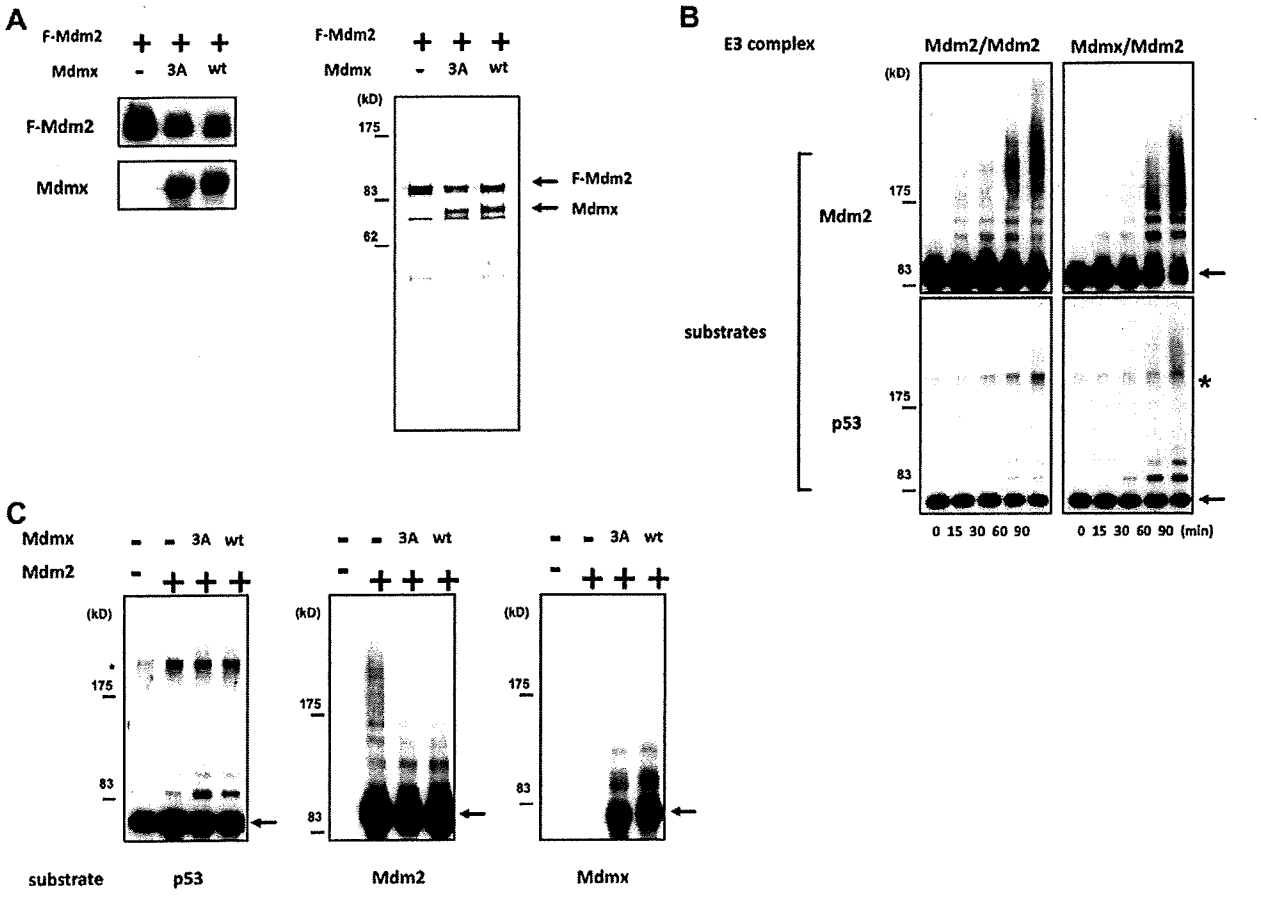

Fig. 2. Association of Mdmx with Mdm2 augments the activity of Mdm2 to ubiquitinate p53 and inhibits auto-ubiquitination of Mdm2 in vitro. (A) Purification of Mdm2 and the Mdm2/Mdmx complex. Flag-tagged Mdm2 was translated alone, or co-translated with Mdmx-3A or wild-type Mdmx in wheat germ lysates, as described in Section 2. The purified proteins were separated by10% SDS–PAGE, and detected by silver staining (right panel), or by Western blotting analyses with anti-Flag antibody (M2) or anti-Mdmx antibody (D-19) (left panel). (B) *In vitro* ubiquitination assays were performed with purified Mdm2 or Mdmx-3A/Mdm2. Ubiquitination reactions were terminated at the indicated times, and the extent of p53 ubiquitination and Mdm2 auto-ubiquitination was evaluated by Western blot analyses with anti-Flag antibody or anti-p53 antibody. The position of non-ubiquitinated substrates is designated by arrows. (C) In vitro ubiquitination assays were performed as described in (B), and the ubiquitination reactions were terminated after 30 min. Ubiquitination of Mdmx, p53, and Mdm2 was evaluated by Western blot analyses.

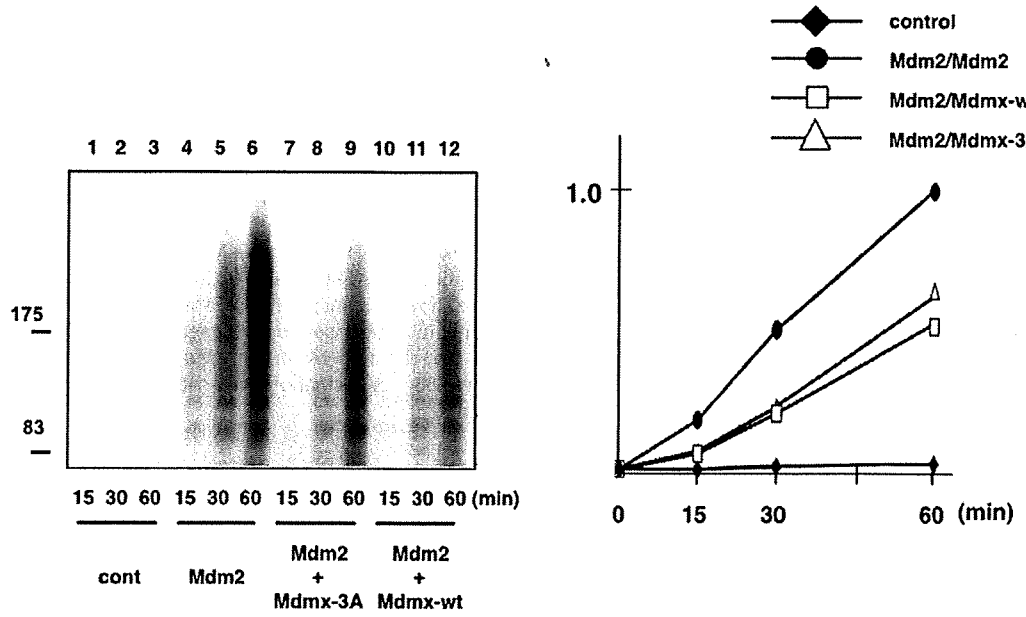

Fig. 3. In vitro ubiquitination reaction was performed as described in Fig. 2C, except that ^{125}I-labeled ubiquitin was included in the reaction. (left panel) Ubiquitinated Mdm2 or Mdm2/Mdmx was separated by 10% SDS–PAGE, and detected by autoradiography. Note that the ladder represents a mixture of ubiqutination of Mdm2 and Mdmx in lanes 7–12 (left panel). Levels of the ubiquitination were quantified and relative levels of ubiquitination were plotted (right panel).

^{125}I-labeled ubiquitin. Quantification of ubiquitin attached to the enzymatic complexes demonstrated that the auto-ubiquitination of the Mdm2 was indeed hindered by the complex formation with either wild-type Mdmx or Mdmx-3A (Fig. 3). Thus, the complex formation of Mdm2 with Mdmx affects the preference for the substrate of the Mdm2 ubiquitin ligase.

3.5. Mdmx stimulates Mdm2-dependent mono-ubiquitination of p53

It has been documented that poly-ubiquitination of p53 induces its degradation, while its mono-ubiquitnation stimulates nuclear export of p53 [33]. Because Mdmx does not significantly contribute to p53 degradation [34], we attempted to determine whether Mdmx stimulates mono-ubiquitination of p53 rather than its poly-ubiquitination. Mdm2 and p53 were introduced into H1299 cells together with His-Ub-K7R, $(His)_6$-tagged mutant ubiquitin which is not capable of forming a ladder of poly-ubiquitination due to arginine substitution in all seven lysine residues [29]. Subsequently, His-Ub-K7R was purified from lysates that were prepared from transfected cells, and p53 conjugated with His-Ub-7KR was detected by Western blot analyses with anti-p53 antibody. The introduction of wild-type Mdmx augmented mono-ubiquitination of p53 (Fig. 4, lane 2), and the Mdmx-3A mutation further enhanced the p53 mono-ubiquitination (Fig. 4, lane 3).

In order to determine whether Mdmx stimulates Mdm2-dependent mono-ubiquitination of p53 in vitro as well as in vivo, methylated ubiquitin was used instead of wild-type ubiquitin in in vitro ubiquitination assays. Indeed, the Mdmx/Mdm2 complex showed a stronger activity for p53 mono-ubiquitination than the homomeric Mdm2 (Fig. S3). Thus, the formation of a complex with Mdmx augments the activity of Mdm2 to mono-ubiquitinate p53.

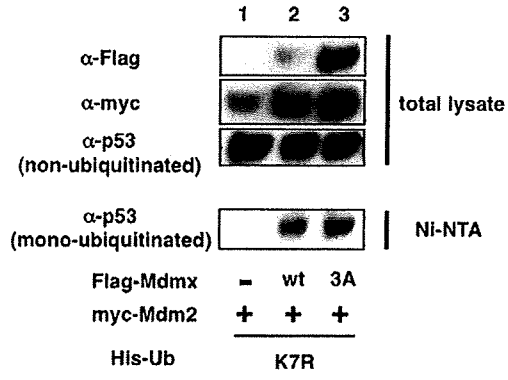

Fig. 4. Mdmx-3A or the control vector was transfected into H1299 cells together with Myc-Mdm2, HA-p53 and the indicated $(His)_6$-tagged ubiquitin K7R mutant. Twenty hours after transfection, cells were lysed with a buffer containing 6 M urea, and normalized lysates that contain equal amounts of non-ubiquitinated p53 were used to purify His-tagged ubiquitin on Ni-NTA agarose (QIAGEN). Ubiquitinated p53 was detected by Western blot analysis with anti-p53 antibody (DO-1).

4. Discussion

In this report, we demonstrated that wild-type Mdmx as well as its non-phosphorylatable mutant cooperates with Mdm2 to stimulate ubiquitination of p53 both in vivo and in vitro. In agreement with our observation, it was reported that Mdmx enhances the activity of Mdm2 as a ubiquitin ligase in vitro [35]. Mdmx complements the catalytic function of mutant Mdm2 proteins that are deficient in the enzymatic activity as a ubiquitin ligase [23–25] and Mdmx/Mdm2 hetero-RING complexes exhibit a greater E3 ligase activity than homomeric Mdm2 [36]. Such effects of Mdmx on Mdm2 should enhance Mdm2-dependent ubiquitination of p53, consistent with the role of Mdmx as an inhibitor of p53.

It was previously reported that Mdmx augments not only auto-ubiquitination of Mdm2 but also the ubiquitin ligase activity of Mdm2 toward p53 [35] in in vitro assays. However, auto-ubiquitination of the Mdm2 ubiquitin ligase negatively affects its activity because poly-ubiquitinated Mdm2 is targeted for proteasome-mediated degradation. Therefore, enhanced ubiquitinase activity of Mdm2 by Mdmx may not be translated into efficient stimulation of p53 ubiquitination if the association of Mdmx to Mdm2 simultaneously leads to stimulation of self-destruction of Mdm2. Our

observation that Mdmx inhibits poly-ubiquitination of Mdm2 while it stimulates p53 ubiquitination may attribute to a mechanism by which Mdmx stimulates Mdm2-dependent p53 ubiquitination without enhanced destruction of Mdm2, thus providing the molecular basis of how Mdmx cooperates with Mdm2 to inhibit p53 activity.

Recently Linke et al. reported the crystal structure of the heterodimer of Mdmx/Mdm2 RING domain, and proposed a model that favors transfer of ubiquitin to Mdmx that does not interact with E2 [37]. This can explain why Mdm2 is not extensively ubiquitinated in the Mdmx/Mdm2 heteromeric complex, thus providing mechanistic basis for reduced ubiquitination of Mdm2 in the Mdmx/Mdm2 complex (Fig. 2). It is noteworthy that, in in vitro ubiquitination assays, the levels of Mdm2 ubiquitination in the homomeric Mdm2 are higher than combined levels of ubiquitination of Mdm2 and Mdmx in the heteromeric complex (Fig. 3). Therefore, it is likely that Mdmx is relatively resistant to ubiquitination by bound Mdm2, unless Mdmx undergoes specific modification such as phosphorylation [27].

It is not clear at this moment how Mdmx stimulates Mdm2-mediated ubiquitination of p53. Mdm2 bound to Mdmx may position its catalytic domain more closer to the C-terminal domain of p53 than homomeric Mdm2, resulting in enhanced p53 ubiquitination. Alternatively, Mdm2 or Mdmx may compete with p53 as a substrate for Mdm2, and relative resistance of Mdmx against ubiquitination by bound Mdm2 may translate into facilitated p53 ubiquitination. Presumably, these two possibilities are not mutually exclusive, and combined effects of Mdmx on Mdm2-mediated ubiquitination may serve to stimulate ubiquitination and inactivation of p53.

Acknowledgements

We thank Aart Jochemsen for helpful suggestions. The His-ubiquitin expression plasmids were kind gifts from Wei Gu. We thank Kenji Kashima and Chihiro Ohtsubo for experimental assistance. This work was supported by a Grant-in-Aid for Scientific Research from the Ministry of Education, Culture, Sports, Science and Technology of Japan (Y.T and K.O.), a Grant-in-Aid for Third Term Comprehensive Control Research for Cancer from the Ministry of Health, Labor and Welfare, Japan (Y.T.), and the Foundation for Promotion of Cancer Research (K.O.).

Appendix A. Supplementary data

Supplementary data associated with this article can be found, in the online version, at doi:10.1016/j.febslet.2009.07.021.

References

[1] Levine, A.J. (1997) P53, the cellular gatekeeper for growth and division. Cell 88, 323–331.
[2] Laptenko, O. and Prives, C. (2006) Transcriptional regulation by p53: one protein, many possibilities. Cell Death Differ. 13, 951–961.
[3] Levine, A.J., Hu, W. and Feng, Z. (2006) The P53 pathway: what questions remain to be explored? Cell Death Differ. 13, 1027–1036.
[4] Oren, M. (2003) Decision making by p53: life, death and cancer. Cell Death Differ. 10, 431–442.
[5] Ko, L.J. and Prives, C. (1996) P53: puzzle and paradigm. Genes Dev. 10, 1054–1072.
[6] Vogelstein, B., Lane, D. and Levine, A.J. (2000) Surfing the p53 network. Nature 408, 307–310.
[7] Lozano, G. and Zambetti, G.P. (2005) What have animal models taught us about the p53 pathway? J. Pathol. 205, 206–220.
[8] Vousden, K.H. and Lu, X. (2002) Live or let die: the cell's response to p53. Nat. Rev. Cancer 2, 594–604.
[9] Olivier, M., Eeles, R., Hollstein, M., Khan, M.A., Harris, C.C. and Hainaut, P. (2002) The IARC TP53 database: new online mutation analysis and recommendations to users. Hum. Mutat. 19, 607–614.
[10] Marine, J.C., Francoz, S., Maetens, M., Wahl, G., Toledo, F. and Lozano, G. (2006) Keeping p53 in check: essential and synergistic functions of Mdm2 and Mdm4. Cell Death Differ. 13, 927–934.
[11] Michael, D. and Oren, M. (2003) The p53-Mdm2 module and the ubiquitin system. Semin. Cancer Biol. 13, 49–58.
[12] Momand, J., Zambetti, G.P., Olson, D.C., George, D. and Levine, A.J. (1992) The mdm-2 oncogene product forms a complex with the p53 protein and inhibits p53-mediated transactivation. Cell 69, 1237–1245.
[13] Oliner, J.D., Pietenpol, J.A., Thiagalingam, S., Gyuris, J., Kinzler, K.W. and Vogelstein, B. (1993) Oncoprotein MDM2 conceals the activation domain of tumour suppressor p53. Nature 362, 857–860.
[14] Ito, A., Lai, C.H., Zhao, X., Saito, S., Hamilton, M.H., Appella, E. and Yao, T.P. (2001) P300/CBP-mediated p53 acetylation is commonly induced by p53-activating agents and inhibited by MDM2. Embo J. 20, 1331–1340.
[15] Kobet, E., Zeng, X., Zhu, Y., Keller, D. and Lu, H. (2000) MDM2 inhibits p300-mediated p53 acetylation and activation by forming a ternary complex with the two proteins. Proc. Natl. Acad. Sci. USA 97, 12547–12552.
[16] Joazeiro, C.A. and Weissman, A.M. (2000) RING finger proteins: mediators of ubiquitin ligase activity. Cell 102, 549–552.
[17] Fang, S., Jensen, J.P., Ludwig, R.L., Vousden, K.H. and Weissman, A.M. (2000) Mdm2 is a RING finger-dependent ubiquitin protein ligase for itself and p53. J. Biol. Chem. 275, 8945–8951.
[18] Honda, R. and Yasuda, H. (2000) Activity of MDM2, a ubiquitin ligase, toward p53 or itself is dependent on the RING finger domain of the ligase. Oncogene 19, 1473–1476.
[19] Honda, R., Tanaka, H. and Yasuda, H. (1997) Oncoprotein MDM2 is a ubiquitin ligase E3 for tumor suppressor p53. FEBS Lett. 420, 25–27.
[20] Tanimura, S., Ohtsuka, S., Mitsui, K., Shirouzu, K., Yoshimura, A. and Ohtsubo, M. (1999) MDM2 interacts with MDMX through their RING finger domains. FEBS Lett. 447, 5–9.
[21] Sharp, D.A., Kratowicz, S.A., Sank, M.J. and George, D.L. (1999) Stabilization of the MDM2 oncoprotein by interaction with the structurally related MDMX protein. J. Biol. Chem. 274, 38189–38196.
[22] Stad, R., Little, N.A., Xirodimas, D.P., Frenk, R., van der Eb, A.J., Lane, D.P., Saville, M.K. and Jochemsen, A.G. (2001) Mdmx stabilizes p53 and Mdm2 via two distinct mechanisms. EMBO Rep. 2, 1029–1034.
[23] Singh, R.K., Iyappan, S. and Scheffner, M. (2007) Hetero-oligomerization with MdmX rescues the ubiquitin/Nedd8 ligase activity of RING finger mutants of Mdm2. J. Biol. Chem. 282, 10901–10907.
[24] Uldrijan, S., Pannekoek, W.J. and Vousden, K.H. (2007) An essential function of the extreme C-terminus of MDM2 can be provided by MDMX. Embo J. 26, 102–112.
[25] Poyurovsky, M.V., Priest, C., Kentsis, A., Borden, K.L., Pan, Z.Q., Pavletich, N. and Prives, C. (2007) The Mdm2 RING domain C-terminus is required for supramolecular assembly and ubiquitin ligase activity. Embo J. 26, 90–101.
[26] Carter, S., Bischof, O., Dejean, A. and Vousden, K.H. (2007) C-terminal modifications regulate MDM2 dissociation and nuclear export of p53. Nat. Cell Biol. 9, 428–435.
[27] Okamoto, K., Kashima, K., Pereg, Y., Ishida, M., Yamazaki, S., Nota, A., Teunisse, A., Migliorini, D., Kitabayashi, I., Marine, J.C., Prives, C., Shiloh, Y., Jochemsen, A.G. and Taya, Y. (2005) DNA damage-induced phosphorylation of MdmX at serine 367 activates p53 by targeting MdmX for Mdm2-dependent degradation. Mol. Cell Biol. 25, 9608–9620.
[28] de Graaf, P., Little, N.A., Ramos, Y.F., Meulmeester, E., Letteboer, S.J. and Jochemsen, A.G. (2003) Hdmx protein stability is regulated by the ubiquitin ligase activity of Mdm2. J. Biol. Chem. 278, 38315–38324.
[29] Li, M., Brooks, C.L., Wu-Baer, F., Chen, D., Baer, R. and Gu, W. (2003) Mono- versus polyubiquitination: differential control of p53 fate by Mdm2. Science 302, 1972–1975.
[30] Ohtsubo, C., Shiokawa, D., Kodama, M., Gaiddon, C., Nakagama, H., Jochemsen, A.G., Taya, Y. and Okamoto, K. (2009) Cytoplasmic tethering is involved in synergistic inhibition of p53 by Mdmx and Mdm2. Cancer Sci.
[31] Gu, J., Nie, L., Wiederschain, D. and Yuan, Z.M. (2001) Identification of p53 sequence elements that are required for MDM2-mediated nuclear export. Mol. Cell Biol. 21, 8533–8546.
[32] Lohrum, M.A., Woods, D.B., Ludwig, R.L., Balint, E. and Vousden, K.H. (2001) C-terminal ubiquitination of p53 contributes to nuclear export. Mol. Cell Biol. 21, 8521–8532.
[33] Shmueli, A. and Oren, M. (2004) Regulation of p53 by Mdm2: fate is in the numbers. Mol. Cell 13, 4–5.
[34] Toledo, F., Krummel, K.A., Lee, C.J., Liu, C.W., Rodewald, L.W., Tang, M. and Wahl, G.M. (2006) A mouse p53 mutant lacking the proline-rich domain rescues Mdm4 deficiency and provides insight into the Mdm2-Mdm4-p53 regulatory network. Cancer Cell 9, 273–285.
[35] Linares, L.K., Hengstermann, A., Ciechanover, A., Muller, S. and Scheffner, M. (2003) HdmX stimulates Hdm2-mediated ubiquitination and degradation of p53. Proc. Natl. Acad. Sci. USA 100, 12009–12014.
[36] Kawai, H., Lopez-Pajares, V., Kim, M.M., Wiederschain, D. and Yuan, Z.M. (2007) RING domain-mediated interaction is a requirement for MDM2's E3 ligase activity. Cancer Res. 67, 6026–6030.
[37] Linke, K., Mace, P.D., Smith, C.A., Vaux, D.L., Silke, J. and Day, C.L. (2008) Structure of the MDM2/MDMX RING domain heterodimer reveals dimerization is required for their ubiquitylation in trans. Cell Death Differ.

Int J Hematol (2009) 89:470–481
DOI 10.1007/s12185-009-0299-0

ORIGINAL ARTICLE

Possible involvement of RasGRP4 in leukemogenesis

Naoko Watanabe-Okochi · Toshihiko Oki · Yukiko Komeno · Naoko Kato · Koichiro Yuji · Ryoichi Ono · Yuka Harada · Hironori Harada · Yasuhide Hayashi · Hideaki Nakajima · Tetsuya Nosaka · Jiro Kitaura · Toshio Kitamura

Received: 25 January 2009 / Revised: 24 February 2009 / Accepted: 8 March 2009 / Published online: 7 April 2009

Abstract It is now conceivable that leukemogenesis requires two types of mutations, class I and class II mutations. We previously established a mouse bone marrow-derived HF6, an IL-3-dependent cell line, that was immortalized by a class II mutation MLL/SEPT6 and can be fully transformed by class I mutations such as FLT3 mutants. To understand the molecular mechanism of leukemogenesis, particularly progression of myelodysplastic syndrome (MDS) to acute leukemia, we made cDNA libraries from the samples of patients and screened them by expression-cloning to detect class I mutations that render HF6 cells factor-independent. We identified RasGRP4, an activator of Ras, as a candidate for class I mutation from three of six patients (MDS/MPD = 1, MDS-RA = 1, MDS/AML = 2, CMMoL/AML = 1 and AML-M2 = 1). To investigate the potential roles of RasGRP4 in leukemogenesis, we tested its in vivo effect in a mouse bone marrow transplantation (BMT) model. C57BL/6J mice transplanted with RasGRP4-transduced primary bone marrow cells died of T cell leukemia, myeloid leukemia, or myeloid leukemia with T cell leukemia. To further examine if the combination of class I and class II mutations accelerated leukemic transformation, we performed a mouse BMT model in which both AML1 mutant (S291fsX300) and RasGRP4 were transduced into bone marrow cells. The double transduction led to early onset of T cell leukemia but not of AML in the transplanted mice when compared to transduction of RasGRP4 alone. Thus, we have identified RasGRP4 as a gene potentially involved in leukemogenesis and suggest that RasGRP4 cooperates with AML1 mutations in T cell leukemogenesis as a class I mutation.

Keywords RasGRP4 · AML1 · Class I mutation · Leukemogenesis · cDNA library

Electronic supplementary material The online version of this article (doi:10.1007/s12185-009-0299-0) contains supplementary material, which is available to authorized users.

N. Watanabe-Okochi · T. Oki · Y. Komeno · N. Kato · H. Nakajima · J. Kitaura · T. Kitamura (✉)
Division of Cellular Therapy, Advanced Clinical Research Center, The Institute of Medical Science, The University of Tokyo, 4-6-1 Shirokanedai, Minato-ku, Tokyo 108-8639, Japan
e-mail: kitamura@ims.u-tokyo.ac.jp

K. Yuji
Division of Molecular Therapy, Advanced Clinical Research Center, The Institute of Medical Science, The University of Tokyo, Tokyo, Japan

R. Ono · T. Nosaka
Department of Microbiology, Mie University Graduate School of Medicine, Tsu-shi, Japan

Y. Harada
International Radiation Information Center, Research Institute for Radiation Biology and Medicine, Hiroshima University, Hiroshima, Japan

H. Harada
Department of Hematology and Oncology, Research Institute for Radiation Biology and Medicine, Hiroshima University, Hiroshima, Japan

Y. Hayashi
Department of Hematology/Oncology, Gunma Children's Medical Center, Shibukawa, Japan

1 Introduction

Various chromosome translocations and gene mutations were known to participate in leukemogenesis. Recently, it was recognized that multiple gene alterations are required

for leukemogenesis; coexistence of chromosomal translocations and gene mutations are frequently found in the same patient. There are some frequent combinations including c-Kit mutations and AML1/ETO [1–6], c-Kit mutations and inv(16) [1, 5–7], Ras mutations and AML1 point mutations [8, 9], FLT3-ITD and AML1 point mutations [10, 11], FLT3 mutations and PML-RARα [12–16], MLL rearrangement and FLT3-TKD [17], MLL rearrangement and Ras mutations [18], and FLT3-ITD and NPM1 mutations [19]. Interestingly, on the other hand, RAS and FLT3 mutations, which are detected in about 50% of patients with de novo AML, are negatively associated with each other [20, 21]. In mice models, while expression of PML/RARα in transgenic mice caused a nonfatal myeloproliferative syndrome, transplantation of bone marrow cells obtained from PML/RARα transgenic mice retrovirally transduced with FLT3-ITD resulted in development of an APL-like disease in a short latency [22]. Two step leukemogenesis was also suggested by an in vitro culture system of human hematopoietic cells [23]. Based on these findings, leukemia-related mutations are classified into two groups, class I and class II mutations. Class I mutations include activating mutations of tyrosine kinases and a small GTPase Ras or inactivation of apoptosis-related molecule, and these mutations induce cell proliferation or block apoptosis. On the other hand, class II mutations include dominant negative mutations of transcription factors involved in differentiation of hematopoietic cells, such as AML1/ETO, PML/RARa, or constitutively activated mutations of chromosome remodeling factors such as MLL-related fusion genes [24]. Indeed, it has been reported that a combination of class I and II mutations such as PML/RARα plus FLT3-ITD [22], AML1/ETO plus FLT3 mutation [25], AML1/EVI1 plus BCR/ABL [26], MLL/SEPT6 plus FLT3 mutation [27], K-ras plus PML/RARα [28] induced AML in a mouse BMT model, while either class I or II mutation alone led to, myeloproliferative disorders (MPD) or MDS like disease, not leukemia [22–28].

To identify class I mutations from patients with MDS/AML, MPD, or AML, we used retrovirus-mediated expression cloning; cDNA libraries from patients' samples were constructed and retrovirally transfected into an IL-3-dependent myeloid cell line, HF6, immortalized by a class II mutation MLL/SEPT6 [27]. We searched for class I mutations that abrogate IL-3 dependency of HF6 and we identified RasGRP4 as a candidate gene from three different libraries (MDS/MPD = 1, MDS/AML = 1, MDS-RA = 1). In addition, FLT3-ITD was identified in a patient with MDS/AML.

RasGRP4 belongs to a family of guanine nucleotide-exchange factors (RasGRP1-4) that positively regulate Ras and related small GTPases, and is mainly expressed in myeloid cells and mast cells [29, 30]. RasGRP4 appears to act downstream of the tyrosine kinase receptor c-Kit/CD117 [30]. RasGRP4 is located on 19q13.1 and alterations of this site have been found in several cancers (the "Cancer Chromosomes" at the NCI web site), and was previously isolated by expression cloning from cytogenetically normal AML patients using the focus-forming assay of NIH3T3 cells [29]. In the present study, we isolated RasGRP4 using expression cloning as a gene that fully transforms IL-3-dependent HF6 cells, and investigated the effect of RasGRP4 overexpression in a mouse BMT model and implicated RasGRP4 in leukemogenesis.

2 Materials and methods

2.1 Cell lines and cell culture

A mouse pro-B line Ba/F3 was maintained in RPMI1640/10% fetal bovine serum (FBS) containing 1 ng/ml recombinant mouse IL-3 (obtained from R & D systems). HF6, which had been established by introducing MLL/SEPT6 into mouse bone marrow cells, was maintained in RPMI1640/10% FBS containing 10 ng/ml mouse IL-3 as described [27].

2.2 Screening of cDNA libraries

Complementary cDNA libraries were generated from patients leukemic or MDS cells (MDS/MPD = 1, MDS/AML = 2, CMMoL/AML = 1, MDS-RA = 1, AML-M2 = 1) as described [31]. MDS or leukemic cells of these patients did not harbor recurrent chromosomal translocations involving AML1 or MLL. One patient with AML-M2 did not display t(8;21). The point mutations of AML1 were not screened. Recombinant retroviruses were generated by transient transfection using an ecotropic packaging cell line PLAT-E as described with minor modifications [32]. Bone marrow or peripheral blood samples of patients were taken under the experimental procedure approved by the ethical committees of our institute (approve no. 20-9).

We introduced each cDNA library into two IL-3-dependent cell lines Ba/F3 and HF6. After transduction with the cDNA library, the transduced cells were seeded into 96-well plates in the absence of IL-3, and factor independent clones were isolated. To identify the cDNA that confers factor independency on Ba/F3 or HF6, genomic DNA of the factor independent clones were purified and integrated cDNAs were isolated and sequenced.

2.3 Vector construction

cDNAs for human RasGRP4 were cloned from cDNA libraries of MDS/MPD patients and normal volunteers using PCR primers: 5′-GGAGCTGAGCCCTACTCTTG-3′

(forward), 5′-AGAGTCTGACGGCAGGACTC-3′ (reverse). We used pfu polymerase (Stratagene, La Jolla, CA) to amplify the coding region of human RasGRP4. We subcloned the PCR products into TOPO vector (Invitrogen, San Diego, CA). Then, the EcoRI fragment carrying RasGRP4 was inserted into the EcoRI sites of pMXs vector [32]. RasGRP4 sequences derived from patients and normal volunteers were not identical to those in the data bases as described in result section. We used an AML1 mutant, S291fsX300, identified from case number 27 among MDS/AML patients [33]. This mutant is hereafter referred to as AML1-S291fs. The AML1-S291fs was inserted upstream of the IRES-EGFP cassette of a retrovirus vector pMYs-IG [32] to generate pMYs-AML1-S291fs-IG.

2.4 Expression of RasGRP4 in HF6

To confirm that the isolated RasGRP4 is responsible for factor-independency of HF6, the cells were infected with the retroviruses harboring pMXs-RasGRP4 derived from patients, normal volunteers or an empty vector as a control, and cultured in the absence of IL-3. To investigate the activation of the Ras pathway in the HF6 cells expressing RasGRP4, the transfected cells were lysed in lysis buffer, and lysates were subject to western blot analysis as described with minor modifications [34]. Monoclonal mouse anti-phospho-p44/42 MAPK (Thr^{202}/Tyr^{204}) antibody (Sigma) was used for phosphorylated ERK1/2.

2.5 Bone marrow transplantation

Bone marrow mononuclear cells were isolated and cultured as described [35]. The prestimulated cells were infected for 60 h with the retroviruses harboring pMXs-RasGRP4 derived from a patient with MDS/MPD, pMYs-AML1-S291fs-IG or an empty vector as a control, using six well dishes coated with RetroNectin (Takara Bio, Inc.) according to the manufacturer's recommendations. Then, 0.3–1.2×10^6 of infected bone marrow cells (Ly-5.1) were injected through tail vein into C57BL/6 (Ly-5.2) recipient mice (8–12 weeks of age) which had been administered a sublethal dose of 5.25 Gy total-body γ-irradiation (135Cs). Overall survival of the transplanted mice was analyzed using the Kaplan–Meier-method. All animal studies were approved by the Animal Care Committee of the Institute of Medical Science, The University of Tokyo.

2.6 Analysis of the transplanted mice

Engraftment of bone marrow cells was confirmed by measuring the percentage of Ly-5.1-positive and/or GFP positive cells in peripheral blood obtained every 1–2 months after the transplant. After the morbid mice were euthanized, their tissue samples including peripheral blood (PB), bone marrow (BM), spleen, liver, and kidney were analyzed. Circulating blood cells were counted by automatic blood cell counter KX-21 (Sysmex, Kobe, Japan). Morphology of the peripheral blood cells was evaluated by staining of air-dried smears with Hemacolor (Merck). Tissues were fixed in 10% buffered formalin, embedded in paraffin, sectioned, and stained with hematoxylin and eosin (H & E). Cytospin preparations of bone marrow and spleen cells were also stained with Hemacolor. The percentage of blasts, myelocytes, neutrophils, monocytes, lymphocytes, and erythroblasts was estimated by examination of at least 200 cells. To assess whether the leukemic cells were transplantable, 2×10^5–1×10^6 total BM cells including blasts were injected into the tail veins of sublethally irradiated mice. A total of two or three recipient mice were used for each serial transplantation.

2.7 Flow cytometric analysis

Peripheral blood or single-cell suspensions of bone marrow and spleen were stained with the following phycoerythrin (PE)-conjugated monoclonal antibodies: Ly-5.1, Gr-1, CD11b, B220, CD3, CD4, CD8, CD41, c-Kit, Sca-1, CD34, and Ter-119. Then, flow cytometric analysis was performed as described [35].

2.8 RT-PCR

To confirm expression of human RasGRP4, total RNA was extracted from BM cells of transplanted mice using Trizol (Invitrogen, California, USA) and cDNA was prepared with the Superscript II RT kit (Invitrogen, California, USA) and RT-PCR was performed using a 2720 Thermal cycler (Applied Biosystems, Tokyo, Japan). The cDNA was amplified using AmpliTaq Gold (Applied Biosystems by Roche Molecular Systems, Inc., New Jersey. USA). The reaction was subject to one cycle at 95°C for 5 min, 30 cycles of PCR at 95°C for 30 s, 55°C for 30 s, and 72°C for 30 s. All samples were independently analyzed at least three times. The following primer pairs were used: 5′-ACTGGCTGATGCGACACCC-3′ (forward) and 5′-GAGATGGCACTGTGACACAG-3′ (reverse) for human RasGRP4, 5′-ACCACAGTCCATGCCATCAC-3′ (forward) and 5′-TCCACCACCCTGTTGCTGTA -3′ (reverse) for GAPDH.

2.9 Quantitative RT-PCR

To examine expression levels of human RasGRP4 in patients, quantitative RT-PCR was performed. Quantitative RT-PCR was performed using a LightCycler Workflow System (Roche Diagnostics, Mannheim, Germany).

Complementary DNAs derived from bone marrow cells of leukemia or MDS patients as well as normal bone marrow cells were amplified using a SYBR Premix EX Taq (TAKARA). The reaction was subject to one cycle at 95°C for 30 s, 45 cycles of PCR at 95°C for 5 s, 55°C for 10 s, and 72°C for 10 s. All samples were independently analyzed at least three times. The primer pairs for human RasGRP4 and GAPDH were the same as described above. The samples from the patients were obtained under written consents which had been approved by the local ethical committee of each institute or hospital.

2.10 Bubble PCR

Genomic DNA was extracted from BM or spleen cells of transplanted mice and digested with EcoRI, and then the fragments were used for Bubble PCR to identify the integration sites of the retroviruses as described [35]. We confirmed inverse repeat sequence "GGGGGTCTTTCA" as a marker of junction between genomic DNA and retrovirus sequence.

3 Results

3.1 RasGRP4 induces factor-independent growth of HF6

In the screening of cDNA libraries, some wells gave rise to cell growth in the absence of IL-3 from HF6 but not from BaF3 cells. The factor-independent clones were isolated and the cDNAs integrated in the genome DNA were sequenced using PCR. FLT3-ITD was identified in one MDS/AML patient. In addition, RasGRP4 was identified from three different libraries (MDS/MPD = 1, MDS/AML = 1, and MDS-RA = 1). We introduced the isolated RasGRP4 into HF6 to confirm that RasGRP4 was responsible for autonomous growth of HF6 cells (Fig. 1a). In the sequence of RasGRP4 derived from the MDS/MPD, MDS/AML and MDS-RA patients, we found several different amino acids that compared with the sequences in two databases GenBank (accession number AF448437) and GenBank (accession number AY048119) (Table 1). Therefore, we introduced RasGRP4 derived from a patient and two Japanese normal volunteers (normal 1 and 2 in Table 1) into HF6 cells to examine if RasGRP4 from normal volunteers also gives rise to factor-independency. As a result, RasGRP4 from normal volunteers also induced factor-independent growth of HF6, indicating that overexpression of RasGRP4 by itself induced transformation of the cells, independent of some mutations in the amino acid sequence of RasGRP4. While several gene alterations were observed in the samples of patients, we focused on E468K because this change was observed only in a patient with MDS/MPD but not in the sequence derived from the two databases and two normal volunteers (Table 1). However, we did not find any functional importance of the alteration at codon 468 that changes a glutamic acid to a lysine. Moreover, SNPs of this gene are not correlated with lymphoma and leukemia (Y. Nakamura, unpublished results).

To assess the RasGRP4-mediated Ras activation, we examined phosphorylation of ERK1/2 using HF6-cells-transduced RasGRP4. Stimulation with IL-3 induced much stronger phosphorylation of ERK1/2 in the HF6 cells expressing RasGRP4 when compared with parent HF6 cells (Fig. 1b, lanes 6–8). Although we did not observe enhanced phosphorylation of ERK1/2 in the cells overexpressing RasGRP4 without IL-3 (Fig. 1b, lane 5), we assume that non-detectable enhancement of ERK1/2 was

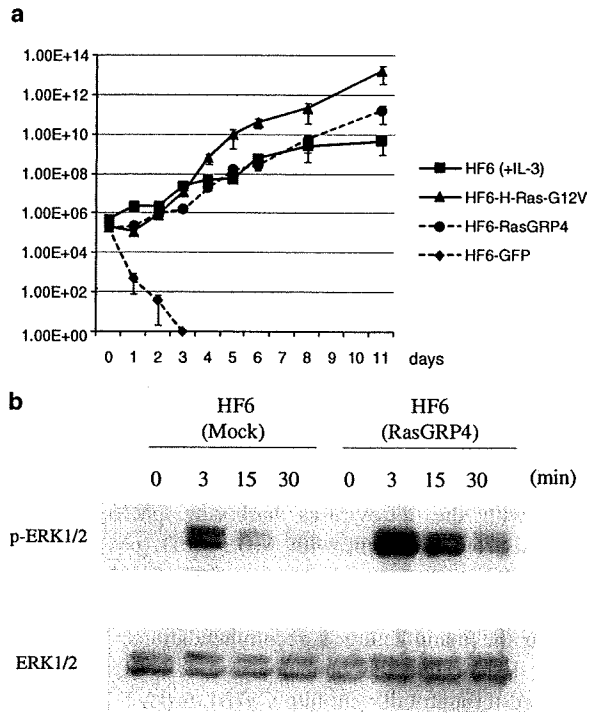

Fig. 1 RasGRP4 conferred factor independency on HF6. **a** HF6 cells expressing the H-Ras-G12V, RasGRP4 and GFP vector were deprived of IL-3, and cells were counted by trypan blue exclusion. The parental HF6 cells in the presence of IL-3 (10 ng/mL) were counted as same. **b** Stimulation with IL-3 induced strong phosphorylation of ERK1/2 in the HF6 cells expressing RasGRP4. Phosphorylation of ERK1/2 (pERK1/2) was examined in HF6 cells transfected with RasGRP4 or empty by western blot analysis using anti-phospho-p44/42 MAPK (Thr^{202}/Tyr^{204}) Ab. Loading amount was estimated by re-probing immunoblots with Abs specific for ERK1/2. The transfected HF6 cells were washed with PBS twice and cultured in RPMI1640/10% FBS without IL-3 for 4 h. Then, some of cells were collected and lysed (*lanes 1 and 5*). The remained cells were stimulated with IL-3 (100 ng/mL) for the indicated period and collected and lysed (*lanes 2–4*, and *6–8*)

Table 1 Polymorphism of RasGRP4

Position of amino acid	AF448437	AY048119	Patient 1 (MDS/MPD)	Patient 2 (MDS/AML)	Patient 3 (MDS-RA)	Normal 1	Normal 2
18	T	T	T	I	T	T	I
120	Q	L	Q	Q	Q	Q	Q
261	R	C	R	R	R	R	R
468	E	E	K	E	E	E	E
541	H	H	H	H	H	H	Y
671	L	P	P	L	L	L	L

enough to induce factor-independent growth of HF6. Only weak activation of the signaling molecule, even non-detectable in biochemical experiments, sometimes induces autonomous cell growth.

3.2 RasGRP4 induced myeloid leukemia and T cell leukemia in mice

We further examined if overexpression of RasGRP4 induced leukemia in a mouse BMT model. We confirmed expression of human RasGRP4 in BM cells of transplanted mice by RT-PCR (Fig. 2a). Transduction of RasGRP4 (E468K) induced myeloid and/or T cell leukemia with various phenotypes, and the transplanted mice died within 2–8 months after the transplantation (Fig. 2b). For example, a mouse (ID 402) died of T cell leukemia with thymoma (weight of thymus was 1,416 mg) and hepatosplenomegaly on day 252 after the transplantation. Leukemic cells showed a CD4- and CD8-double-positive phenotype (Fig. 3). One other mouse developed a similar disease (ID 401). Unfortunately, this mouse died on day 224 before we found out. Therefore, we could only confirm hepatosplenomegaly and a giant thymoma after the death. Two mice (ID 407 and 408) died of AML with hepatosplenomegaly on days 47 and 66 after the transplantation. Severe leukocytosis, anemia and thrombocytopenia were observed in a mouse (ID 408), but severe pancytopenia was observed in the other mouse (ID 407). Leukemic cells of the mouse (ID 408) in bone marrow and thymus uniformly expressed Gr1, CD11b, and B220 on their surfaces (Fig. 3). Four of the transplanted mice (ID 403, 404, 405 and 406) developed both myeloid and T cell leukemia with hepatosplenomegaly, and in some cases, thymoma (ID 404, 405 and 406). In the mouse ID 404, both myeloid and T cell leukemia cells were observed in the bone marrow, while peripheral blood was occupied with myeloid leukemia and thymus was occupied with T cell leukemia (Figs. 3, 4). In summary, two mice died of AML after a short latency (days 47 and 66), two mice died of T cell leukemia after a long latency (days 224 and 252), and four mice died of AML and T cell leukemia (days 76, 83, 129, and 248). The

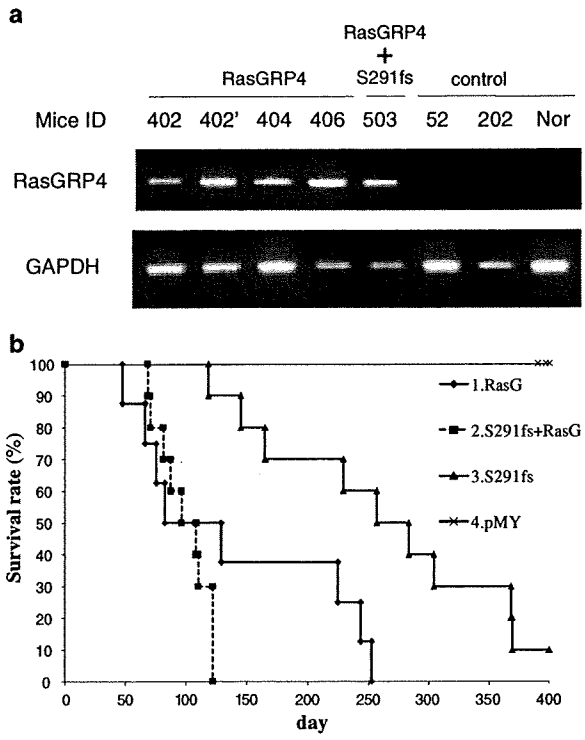

Fig. 2 Co-transduction of RasGRP4 and AML1-S291fs led to early onset of leukemia. **a** Expression of retrovirally introduced RasGRP4 in BM cells. Total RNA from BM cells of transplanted mice were extracted, and the derived cDNAs were subjected to RT-PCR. Mice IDs were shown on the top of the panel. ID 402′ is a second recipient of ID 402. Controls are AML1-S291fs (ID 52), empty vector (ID 202), and normal mouse (Nor). **b** Kaplan–Meier analysis for the survival of mice transplanted with RasGRP4, AML1-S291fs, and double-transduced BM cells. Average survival of RasGRP4 alone (139.8 days) was not significantly different when compared with double transduced mice (101.5 days) ($P = 0.223$, log rank test). Average survival of the double transduced mice (101.5 days) was significantly shorter than that of AML1-S291fs-transduced mice (263.6 days) ($P = 0.00003$, log rank test). RasGRP4 ($n = 8$), AML1-S291fs ($n = 10$), RasGRP4 + AML1-S291fs ($n = 11$), mock ($n = 16$) transduced bone marrow cells were transplanted to mice

details of individual mice are shown in Table 2 and Fig. 5. To assess whether the leukemic cells were transplantable, 2×10^5–1×10^6 total BM cells including blasts were

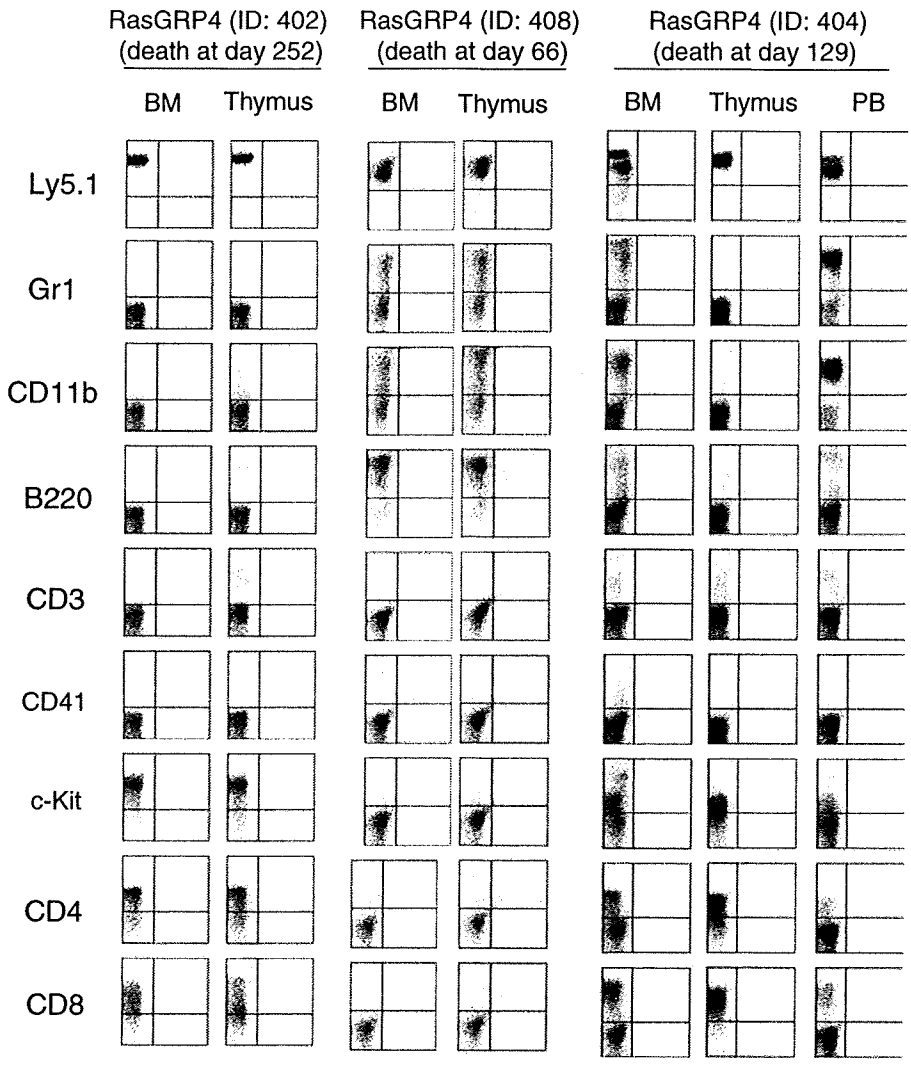

Fig. 3 RasGRP4 induced T cell leukemia and myeloid leukemia in the BMT model. The *dot plots* show Ly5.1, Gr-1, CD11b, B220, CD3, CD41, c-kit, CD4, or CD8 expression detected by corresponding PE-conjugated mAb

injected into recipient mice. We confirmed that both T cell leukemia and myeloid leukemia cells were serially transplantable although the phenotypes slightly changed after the serial transplantation (Supplemental Fig. 1).

3.3 Different integration sites were identified from T cell or myeloid leukemia cells derived from an individual mouse

To examine if the T cell and myeloid leukemia cells were derived from different clones or the same clone, we identified the integration sites in genomic DNA samples of thymus, peripheral blood or bone marrow cells. As shown in Table 3, different integration sites were identified from T cell and myeloid leukemia cells derived from an individual mouse, suggesting that T cell and myeloid leukemic cells were derived from different clones.

The integration near the Samsn1 gene was found twice in ID 405 and ID 406. These mice were transplanted on the same day. The integration site was identical among these leukemic cells indicating that leukemic cells of the two cases were derived from a single hematopoietic progenitor. This result suggests that the integration induced expansion of the transduced stem cells during the 3-day-culture period before the transplantation. Indeed, the mice with the integration at Samsn1 site developed AML with the same phenotype (CD11b positive) and similar latencies (83 and 76 days). On the other hand, different T lineage clones grew up in thymus and developed thymoma.

3.4 RasGRP4 cooperates with an AML1 mutant in leukemogenesis

RasGRP4 appears to function downstream of the tyrosine kinase receptor c-Kit/CD117 [30]. High expression of c-kit

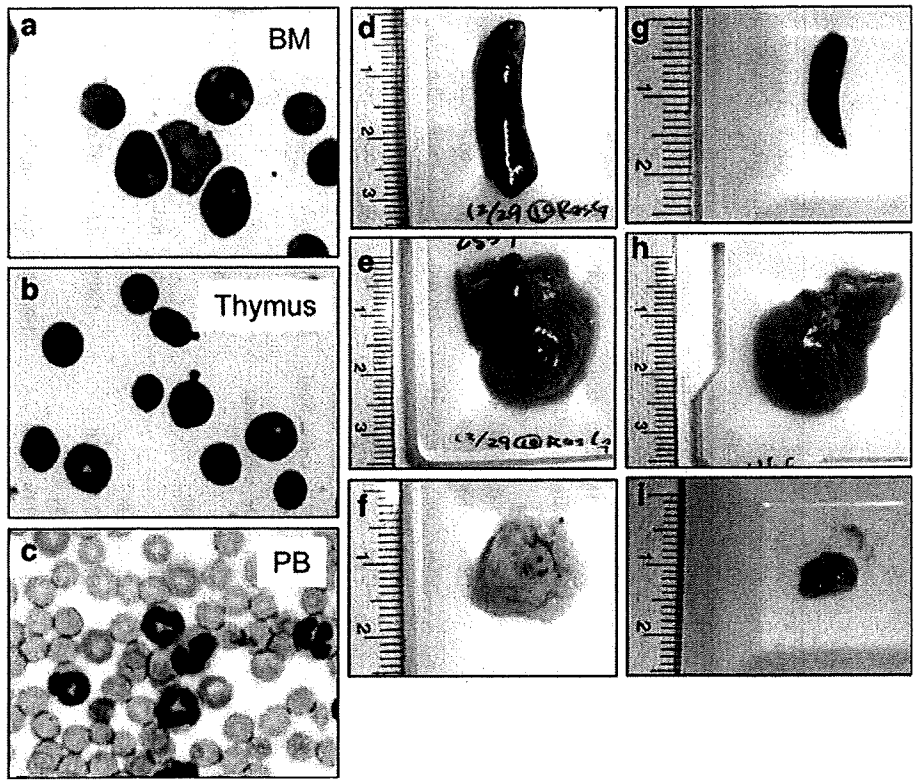

Fig. 4 RasGRP4 induced both of T cell leukemia and myeloid leukemia in the same mouse. Giemsa-stained cells derived from **a** bone marrow, **b** thymus, and **c** peripheral blood obtained from mouse ID 404. Macroscopic findings of **d** spleen, **e** liver, **f** thymus from mice ID 404; *left* **g** spleen, **h** liver, **i** thymus from normal mice; *right* are shown. Images (**a**, **b**, **c**) were obtained with a BH51 microscope and DP12 camera (Olympus, Tokyo, Japan); objective lens, UPlanFl (Olympus); ×1,000

has been found in 60–80% of AML [36] and higher expression is observed in 81.3% of patients with t(8;21) when compared with the patients with other leukemias [2]. Niimi et al. [9] reported that MDS/AML arising from AML1/RUNX1 mutations frequently involves receptor tyrosine kinase (RTK)-RAS signaling pathway activation. We have recently demonstrated that bone marrow cells transduced with AML1 mutants induced MDS-like symptoms after a long latency [35]. Therefore, we also tested if the combination of RasGRP4 and AML1-S291fs, one of the AML1 mutants, induced rapid leukemic transformation in a BMT model. As a result, co-transduction of RasGRP4 and AML1-S291fs led to early death in the transplanted mice (average 101.5 days, $n = 11$) than the expression of RasGRP4 alone (average 139.8 days, $n = 8$) (Fig. 2b). We diagnosed the double-transfected disease mice as T cell leukemia because of enlarged thymus, hepatosplenomegaly, and expansion of blast expressing CD3, CD4, and CD8 in bone marrow, peripheral blood, and thymus (Fig. 6). The onset of T cell leukemia was significantly earlier in the RasGRP4 + AML1 mutant (average 102.7 days, $n = 9$) than RasGRP4 alone (average 238 days, $n = 2$). On the other hand, onset of AML was not significantly changed between RasGRP4 + AML1 mutant (average 96 days, $n = 2$) and RasGRP4 alone (average 56.5 days, $n = 2$) transplanted mice.

3.5 RasGRP4 was overexpressed in some patients with hematological malignancies

We examined expression levels of RasGRP4 in patients with myeloid or T lineage hematological malignancies. As shown in Fig. 7, cells from some patients (T-ALL, AML-M1, MDS-RAEB, MDS-RA, CMMoL) overexpressed RasGRP4.

4 Discussions

We identified RasGRP4 from patients' cDNA libraries as a gene that renders IL-3-dependent HF6 cells factor independent when expressed at high levels via retrovirus-mediated gene transfer. Although we did not find any gain-of-function mutation of RasGRP4 in three patients from whom we identified cDNA for RasGRP4, and we detected high expression of RasGARP4 in only one out of the three patients, it is possible that overexpression or activating mutations are found in patients with malignant diseases including leukemia and MDS. Thus, RasGRP4 is a candidate gene for class I mutations. In addition to RasGRP4, we also identified FLT3-ITD from a patient with MDS/AML, thus showing the feasibility of our functional cloning strategy. The HF6 cells were immortalized by expression

Table 2 Hematological data of the transplanted mice

Gene	Mice ID	GFP (%)	Ly5.1 of BM (%)	Ly5.1 of Thymus (%)	Period from BMT (day)	Spleen weight (mg)	Liver weight (mg)	Thymus weight (mg)	Suefice markers of GFP positive cells	WBC (μL)	Hb (g/dL)	MCV (fL)	Platelet (×1,000/μL)
S291fs	51	27.4	39.8	–	368	153	1,236	–	Gr1, CD11b, CD41, cKit	4,800	6.6	60.0	27.0
S291fs	52	47.8	83.0	–	256	90	1,568	–	Gr1, CD11b, CD41, cKit	4,500	9.9	59.8	38.3
S291fs	54	29.8	45.3	–	304	338	1,812	–	CD11b, CD41, cKit, CD34	1,800	10.4	61.3	4.1
S291fs	55	75.2	83.1	–	165	166	1,574	–	Gr1, CD11b, CD41, cKit,	1,200	4.8	76.4	5.7
S291fs	56	54.9	85.2	–	118	73	1,318	–	CD41, cKit, Sca1, CD34,	2,900	4.5	72.7	4.6
S291fs	57	–	–	–	145	181	1,249	–	–	5,700	2.4		5.1
S291fs	58	72.7	56.5	–	228	225	1,582	–	Gr1, CD11b, CD41, cKit	2,100	9.9	62.7	26.7
S291fs	60	76.3		–	369	186	1,682	–	CD41, c-Kit, CD34	7,500	11.1	66.1	22.2
RasGRP4	402	–	96.5		252	318	1,975		CD4, CD8, c-Kit, Sca1	20,700	12.3	51.9	3.6
				98.9				1,416	CD4, CD8, c-Kit, Sca1				
RasGRP4	403	–	93.5		248	696	2,138		CD41, c-Kit, CD34	8,400	7.2	55.1	0.0
				85.9				92	CD3, CD4, CD8, Sca1				
RasGRP4	404	–	93.9		129	714	2,557		Gr1, CD11b, c-Kit, Sca1, CD4, CD8	282,000	11.7	56.6	3.0
				99.7				777	CD4, CD8, c-Kit, Sca1				
RasGRP4	405	–	91.3		83	1,184	3,699		CD11b	558,900	7.2	57.1	9.9
				98.3				139	CD4, CD8				
RasGRP4	406	–	94.8		76	1,348	2,678		CD11b	96,900	6.6	59.7	1.2
				99.5				609	CD4, CD8				
RasGRP4	407	–	32.0		47	670	4,795		Gr1, CD11b, c-Kit	1,800	4.5	67.6	2.7
				17.1				95	CD3, CD4, CD8				
RasGRP4	408	–	95.7		66	1,110	4,155		Gr1, CD11b, B220	108,900	5.1	104.0	3.9
				93.5				202	Gr1, CD11b, B220				
S291fs + RasGRP4	503	92.1	92.1		96	1,180	6,065		CD3, CD4, CD8	33,600	10.3	64.5	9.3
		95.0		95.0				112	CD3, CD4, CD8				
S291fs + RasGRP4	507	–	–		68	302	–		CD3, CD4, CD8				
				–				805	CD3, CD4, CD8				
S291fs + RasGRP4	513	75.8	80.7		130	544	2,784		CD3, CD8	59,500	10.7	68.8	2.2
		83.8		90.9				155	CD3, CD8				

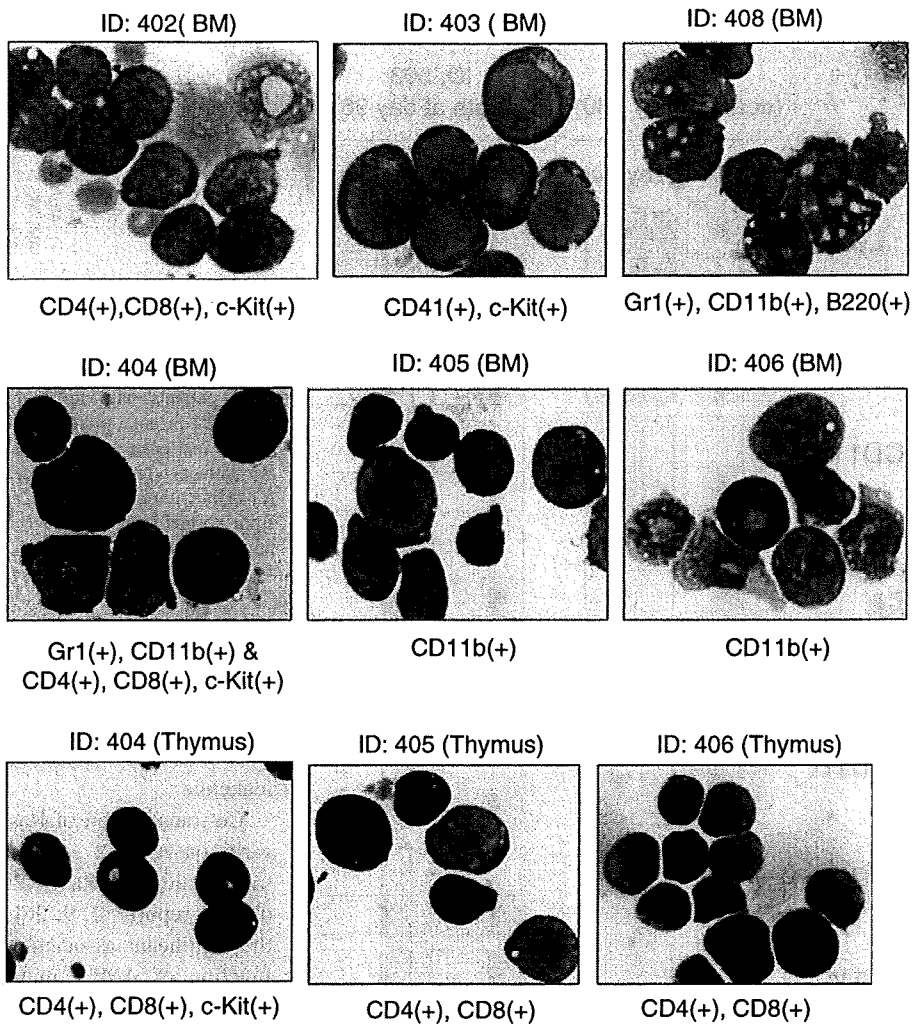

Fig. 5 Morphology of leukemic cells induced by RasGRP4. Giemsa staining photos of the leukemic cells are shown. Mice IDs were shown at *top of the panel*. Surface expression proteins were shown at bottom of the panel. Images were obtained with a BH51 microscope and DP12 camera (Olympus, Tokyo, Japan); objective lens, UPlanFl (Olympus); magnification, ×1,000

Table 3 Retroviral integration sites in the transplanted mice

Mice ID	Sample	Chr. number	Nearest gene	Gene ID	Distance to gene (start or end)	Location	Forward or reverse orientation	RTCGD hits
404	Thymus	10	Bcr	110279	Disrupt CDS	Intron 8	F	0
404	PB	15	Trio	223435	Disrupt CDS	Intron 9	F	3
405	Thymus	14	LOC100042147	100042147	12,962 bp	3′	R	0
405	BM	16	Samsn1	67742	95,998 bp	5′	R	2
406	Thymus	18	LOC100042131	100042131	Disrupt CDS	Exon 2	F	0
406	BM	16	Samsn1	67742	95,998 bp	5′	R	2

of MLL-SEPT6, and can be transformed by oncogenic Ras and Ras-related signals (manuscript in preparation). Therefore, HF6 is a suitable cell line for identification of Ras mutations as well as mutations of Ras-related signaling molecules. On the other hand, Ba/F3 cells can be transformed by STAT5 activation. In addition to these two cell lines, we have developed several other IL-3-dependent bone marrow-derived cell lines immortalized by class II mutations or related molecules (unpublished results). Because these IL-3-dependent cell lines have different signaling profiles, they would be applicable for identification of mutations in a variety of signaling molecules, providing a versatile system for functional cloning of oncogenic mutations.

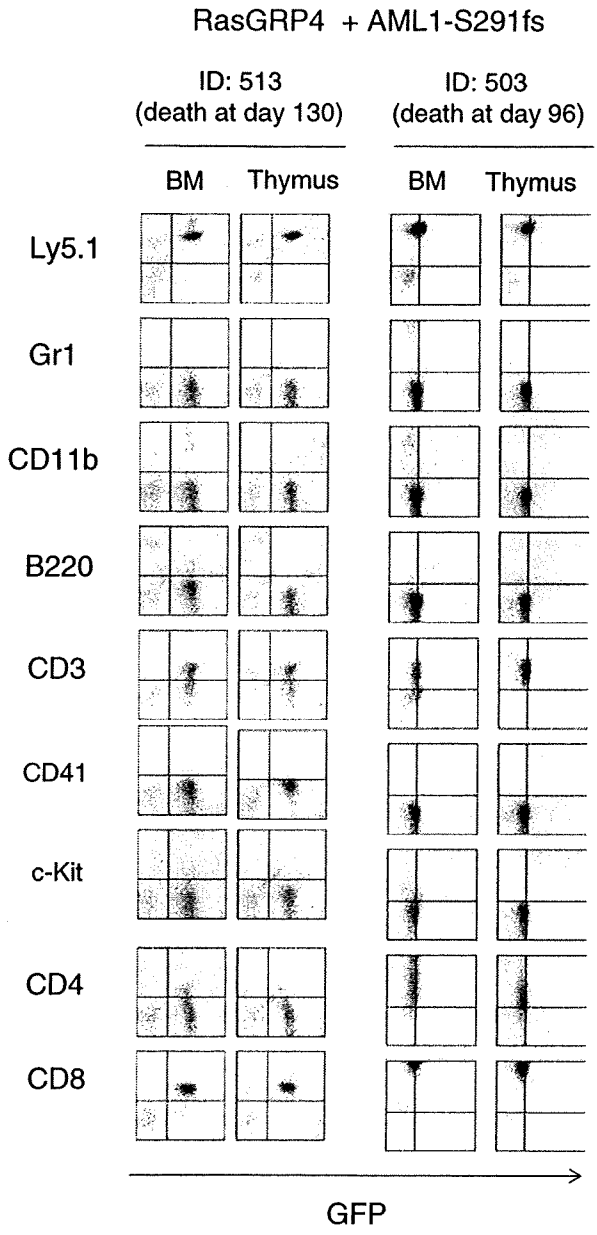

Fig. 6 RasGRP4 and AML1-S291fs induced T cell leukemia in the BMT model. The *dot plots* show Ly5.1, Gr-1, CD11b, B220, CD3, CD41, c-kit, CD4, or CD8 expression detected by corresponding PE-conjugated mAb

Overexpression of RasGRP4-induced T cell leukemia and/or myeloid leukemia in a mouse BMT model. We found that four of eight mice developed both types of leukemia and two mice died of AML after a short latency, while others died of T cell leukemia after a long latency when transplanted with RasGRP4 alone. At present, it is not clear what determines the different phenotypes of leukemia induced by RasGRP4. Although

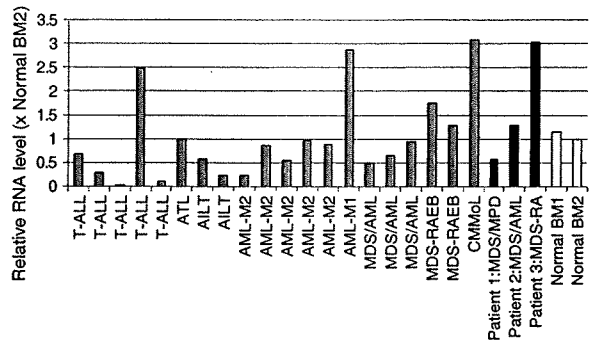

Fig. 7 RasGRP4 was overexpressed in a patient with T-ALL and some patients with myeloid malignancies. Expression levels of RasGRP4 in bone marrow cells derived from patients with hematological malignancies were evaluated by quantitative RT-PCR. *Gray bar* patients with hematological malignancies, *black bar* patients used for cDNA library and identified RasGRP4, *white bar* normal. RNAs from normal bone marrow cells served as a control (RNA level of normal BM2 = 1)

the retrovirus integration site should modify the outcome, so far we did not find any integration that could explain the differing phenotypes of leukemia. Alternatively, it is also possible that types of progenitors transduced with RasGRP4 determine the different phenotypes of leukemia.

Co-transduction of RasGRP4 and AML1-S291fs led to early onset of T cell leukemia as compared with the transduction of RasGRP4 alone. Putting together with clinical reports [2, 9, 36] and our results, we can suggest the significant association of Ras signaling pathway and function of AML1 mutation in leukemogenesis. While AML1 mutations are frequently associated with myeloid leukemia in human patients, they seemed to shorten the latency of T cell leukemia induced by forced expression of RasGRP4 in mouse BMT model. Intriguingly, while RasGRP4 induced c-Kit+/CD3−/CD4+/CD8+ T cell leukemia, combination of RasGRP4 and AML1-S291fs developed more mature T cell leukemia (c-Kit−/CD3+/CD8+/CD4− or CD4+). The reason for this difference is elusive at present. Although we need more cases of BMT mice for confirmation of this difference, AML1-S291fs may also play some roles to induce T cell differentiation in addition to its overall dominant effects on AML1 transcription. In the clinical cases, AML1-LAF4 [37] and AML1-FGA7 [38] were associated with T-ALL, although most of AML1 translocations are associated with myeloid leukemia. Because AML1 is important for transcription of TCR and silencing of CD4, it is possible that AML1-S291fs inhibited the normal ontogeny of T cells, thus accelerating leukemogenic process caused by RasGRP4 in a mice BMT model as a class II mutation that disturbs T cell ontogeny.

Reuther et al. previously isolated RasGRP4 by focus-forming assay of NIH3T3 cells from a patient with AML. This AML-derived RasGRP4 contained a point mutation at codon 620 that changes glutamic acid to lysine at the carboxyl terminus of the protein [29]. However, they found no significant difference in the ability of the AML-derived point mutated RasGRP4 (E620K) or wild-type RasGRP4 (GenBank™ accession number AF448437) in activation of Ras proteins. In our study, we found a gene alteration that induces an amino acid substitution from glutamic acid to lysine at 468 position of RasGRP4 in a patient with MDS/MPD. However, we did not detect a functional difference between RasGRP4 harboring an E468K substitution and RasGRP4 derived from normal volunteers in the ability to abrogate IL-3-dependency of HF6 cells. Moreover, SNPs of this gene are not correlated with lymphoma and leukemia (Y. Nakamura, unpublished results). These results indicate that the sequence difference simply represents a polymorphism or a neutral mutation and has no significant meaning in inducing leukemia. At present, it is not clear whether the sequence alterations in RasGRP4 gene are derived from germ line or somatic mutations.

We found overexpression of RasGRP4 in a patient with T-ALL but it is difficult to conclude the association of RasGRP4 with T-ALL. We also found overexpression of RasGRP4 in some patients with AML-M1, MDS-RAEB, MDS-RA, and CMMoL. The current results suggest that RasGRP4 plays important roles in leukemogenesis in some patients. A clinical study using a large number of patients' samples is required to fully understand the association of RasGRP4 with leukemogenesis.

In summary, we identified RasGRP4 as a candidate gene of class I mutations by our expression cloning strategy based on retrovirus-mediated gene transfer [31, 32, 39]. Although we did not find significant mutations in RasGRP4 derived from patients, overexpression of RasGRP4 confers factor independency on an IL-3 dependent cell line and induced T cell leukemia and myeloid leukemia in a mouse BMT model. Our results indicate possible involvement of RasGRP4 in leukemogenesis.

Acknowledgments We thank Fumi Shibata for technical assistance and Dr. Yusuke Nakamura for the SNPs information of RasGRP4. This work was supported by a grant-in-aid for Cancer Research supported by the Ministry of Health, Labor and Welfare and a grant from the Vehicle Racing Commemorative Foundation.

References

1. Beghini A, Peterlongo P, Ripamonti CB, Larizza L, Cairoli R, Morra E, et al. C-kit mutations in core binding factor leukemias. Blood. 2000;95:726–7.
2. Wang YY, Zhou GB, Yin T, Chen B, Shi JY, Liang WX, et al. AML1-ETO and C-KIT mutation/overexpression in t(8;21) leukemia: implication in stepwise leukemogenesis and response to Gleevec. Proc Natl Acad Sci USA. 2005;102:1104–9. doi: 10.1073/pnas.0408831102.
3. Shimada A, Taki T, Tabuchi K, Tawa A, Horibe K, Tsuchida M, et al. KIT mutations, and not FLT3 internal tandem duplication, are strongly associated with a poor prognosis in pediatric acute myeloid leukemia with t(8;21): a study of the Japanese Childhood AML Cooperative Study Group. Blood. 2006;107:1806–9. doi: 10.1182/blood-2005-08-3408.
4. Yamashita N, Osato M, Huang L, Yanagida M, Kogan SC, Iwasaki M, et al. Haploinsufficiency of Runx1/AML1 promotes myeloid features and leukemogenesis in BXH2 mice. Br J Haematol. 2005;131:495–507. doi:10.1111/j.1365-2141.2005.05793.x.
5. Care RS, Valk PJ, Goodeve AC, Abu-Duhier FM, Geertsma-Kleinekoort WM, Wilson GA, et al. Incidence and prognosis of c-KIT and FLT3 mutations in core binding factor (CBF) acute myeloid leukaemias. Br J Haematol. 2003;121:775–7. doi: 10.1046/j.1365-2141.2003.04362.x.
6. Boissel N, Leroy H, Brethon B, Philippe N, de Botton S, Auvrignon A, et al. Incidence and prognostic impact of c-Kit, FLT3, and Ras gene mutations in core binding factor acute myeloid leukemia (CBF-AML). Leukemia. 2006;20:965–70. doi: 10.1038/sj.leu.2404188.
7. Beghini A, Ripamonti CB, Cairoli R, Cazzaniga G, Colapietro P, Elice F, et al. KIT activating mutations: incidence in adult and pediatric acute myeloid leukemia, and identification of an internal tandem duplication. Haematologica. 2004;89:920–5.
8. Christiansen DH, Andersen MK, Desta F, Pedersen-Bjergaard J. Mutations of genes in the receptor tyrosine kinase (RTK)/RAS-BRAF signal transduction pathway in therapy-related myelodysplasia and acute myeloid leukemia. Leukemia. 2005;19:2232–40. doi:10.1038/sj.leu.2404009.
9. Niimi H, Harada H, Harada Y, Ding Y, Imagawa J, Inaba T, et al. Hyperactivation of the RAS signaling pathway in myelodysplastic syndrome with AML1/RUNX1 point mutations. Leukemia. 2006;20:635–44. doi:10.1038/sj.leu.2404136.
10. Matsuno N, Osato M, Yamashita N, Yanagida M, Nanri T, Fukushima T, et al. Dual mutations in the AML1 and FLT3 genes are associated with leukemogenesis in acute myeloblastic leukemia of the M0 subtype. Leukemia. 2003;17:2492–9. doi: 10.1038/sj.leu.2403160.
11. Roumier C, Eclache V, Imbert M, Davi F, MacIntyre E, Garand R, et al. M0 AML, clinical and biologic features of the disease, including AML1 gene mutations: a report of 59 cases by the Groupe Français d'Hématologie Cellulaire (GFHC) and the Groupe Français de Cytogénétique Hématologique (GFCH). Blood. 2003;101:1277–83. doi:10.1182/blood-2002-05-1474.
12. Callens C, Chevret S, Cayuela JM, Cassinat B, Raffoux E, de Botton S, et al. Prognostic implication of FLT3 and Ras gene mutations in patients with acute promyelocytic leukemia (APL): a retrospective study from the European APL Group. Leukemia. 2005;19:1153–60. doi:10.1038/sj.leu.2403790.
13. Gale RE, Hills R, Pizzey AR, Kottaridis PD, Swirsky D, Gilkes AF, et al. Relationship between FLT3 mutation status, biologic characteristics, and response to targeted therapy in acute promyelocytic leukemia. Blood. 2005;106:3768–76. doi:10.1182/blood-2005-04-1746.
14. Arrigoni P, Beretta C, Silvestri D, Rossi V, Rizzari C, Valsecchi MG, et al. FLT3 internal tandem duplication in childhood acute myeloid leukaemia: association with hyperleucocytosis in acute promyelocytic leukaemia. Br J Haematol. 2003;120:89–92. doi: 10.1046/j.1365-2141.2003.04032.x.
15. Noguera NI, Breccia M, Divona M, Diverio D, Costa V, De Santis S, et al. Alterations of the FLT3 gene in acute

promyelocytic leukemia: association with diagnostic characteristics and analysis of clinical outcome in patients treated with the Italian AIDA protocol. Leukemia. 2002;16:2185–9. doi:10.1038/sj.leu.2402723.
16. Kainz B, Heintel D, Marculescu R, Schwarzinger I, Sperr W, Le T, et al. Variable prognostic value of FLT3 internal tandem duplications in patients with de novo AML and a normal karyotype, t(15;17), t(8;21) or inv(16). Hematol J. 2002;3:283–9. doi:10.1038/sj.thj.6200196.
17. Taketani T, Taki T, Sugita K, Furuichi Y, Ishii E, Hanada R, et al. FLT3 mutations in the activation loop of tyrosine kinase domain are frequently found in infant ALL with MLL rearrangements and pediatric ALL with hyperdiploidy. Blood. 2004;103:1085–8. doi:10.1182/blood-2003-02-0418.
18. Liang DC, Shih LY, Fu JF, Li HY, Wang HI, Hung IJ, et al. K-Ras mutations and N-Ras mutations in childhood acute leukemias with or without mixed-lineage leukemia gene rearrangements. Cancer. 2006;106:950–6. doi:10.1002/cncr.21687.
19. Gale RE, Green C, Allen C, Mead AJ, Burnett AK, Hills RK, et al. The impact of FLT3 internal tandem duplication mutant level, number, size, and interaction with NPM1 mutations in a large cohort of young adult patients with acute myeloid leukemia. Blood. 2008;111:2776–84. doi:10.1182/blood-2007-08-109090.
20. Kiyoi H, Naoe T, Nakano Y, Yokota S, Minami S, Miyawaki S, et al. Prognostic implication of FLT3 and N-RAS gene mutations in acute myeloid leukemia. Blood. 1999;93:3074–80.
21. Stirewalt DL, Kopecky KJ, Meshinchi S, Appelbaum FR, Slovak ML, Willman CL, et al. FLT3, RAS, and TP53 mutations in elderly patients with acute myeloid leukemia. Blood. 2001;97:3589–95. doi:10.1182/blood.V97.11.3589.
22. Kelly LM, Kutok JL, Williams IR, Boulton CL, Amaral SM, Curley DP, et al. PML/RARalpha and FLT3-ITD induce an APL-like disease in a mouse model. Proc Natl Acad Sci USA. 2002;99:8283–8. doi:10.1073/pnas.122233699.
23. Warner JK, Wang JC, Takenaka K, Doulatov S, McKenzie JL, Harrington L, et al. Direct evidence for cooperating genetic events in the leukemic transformation of normal human hematopoietic cells. Leukemia. 2005;19:1794–805. doi:10.1038/sj.leu.2403917.
24. Gilliland DG, Griffin JD. Role of FLT3 in leukemia. Curr Opin Hematol. 2002;9:274–81. doi:10.1097/00062752-200207000-00003.
25. Schessl C, Rawat VP, Cusan M, Deshpande A, Kohl TM, Rosten PM, et al. The AML1-ETO fusion gene and the FLT3 length mutation collaborate in inducing acute leukemia in mice. J Clin Invest. 2005;115:2159–68. doi:10.1172/JCI24225.
26. Cuenco GM, Ren R. Cooperation of BCR-ABL and AML1/MDS1/EVI1 in blocking myeloid differentiation and rapid induction of an acute myelogenous leukemia. Oncogene. 2001;20:8236–48. doi:10.1038/sj.onc.1205095.
27. Ono R, Nakajima H, Ozaki K, Kumagai H, Kawashima T, Taki T, et al. Dimerization of MLL fusion proteins and FLT3 activation synergize to induce multiple-lineage leukemogenesis. J Clin Invest. 2005;115:919–29.
28. Chan IT, Kutok JL, Williams IR, Cohen S, Moore S, Shigematsu H, et al. Oncogenic K-ras cooperates with PML-RAR alpha to induce an acute promyelocytic leukemia-like disease. Blood. 2006;108:1708–15. doi:10.1182/blood-2006-04-015040.
29. Reuther GW, Lambert QT, Rebhun JF, Caligiuri MA, Quilliam LA, Der CJ. RasGRP4 is a novel Ras activator isolated from acute myeloid leukemia. J Biol Chem. 2002;277:30508–14. doi:10.1074/jbc.M111330200.
30. Yang Y, Li L, Wong GW, Krilis SA, Madhusudhan MS, Sali A, et al. RasGRP4, a new mast cell-restricted Ras guanine nucleotide-releasing protein with calcium- and diacylglycerol-binding motifs Identification of defective variants of this signaling protein in asthma, mastocytosis, and mast cell leukemia patients and demonstration of the importance of RasGRP4 in mast cell development and function. J Biol Chem. 2002;277:25756–74. doi:10.1074/jbc.M202575200.
31. Kitamura T, Onishi M, Kinoshita S, Shibuya A, Miyajima A, Nolan GP. Efficient screening of retroviral cDNA expression libraries. Proc Natl Acad Sci USA. 1995;92:9146–50. doi:10.1073/pnas.92.20.9146.
32. Kitamura T, Koshino Y, Shibata F, Oki T, Nakajima H, Nosaka T, et al. Retrovirus-mediated gene transfer and expression cloning: powerful tools in functional genomics. Exp Hematol. 2003;31:1007–14.
33. Harada H, Harada Y, Niimi H, Kyo T, Kimura A, Inaba T. High incidence of somatic mutations in the AML1/RUNX1 gene in myelodysplastic syndrome and low blast percentage myeloid leukemia with myelodysplasia. Blood. 2004;103:2316–24. doi:10.1182/blood-2003-09-3074.
34. Izawa K, Kitaura J, Yamanishi Y, Matsuoka T, Oki T, Shibata F, et al. Functional analysis of activating receptor LMIR4 as a counterpart of inhibitory receptor LMIR3. J Biol Chem. 2007;282:17997–8008. doi:10.1074/jbc.M701100200.
35. Watanabe-Okochi N, Kitaura J, Ono R, Harada H, Harada Y, Komeno Y, et al. AML1 mutations induced MDS and MDS/AML in a mouse BMT model. Blood. 2008;111:4297–308. doi:10.1182/blood-2007-01-068346.
36. Reuss-Borst MA, Bühring HJ, Schmidt H, Müller CA. AML: immunophenotypic heterogeneity and prognostic significance of c-kit expression. Leukemia. 1994;8:258–63.
37. Chinen Y, Taki T, Nishida K, Shimizu D, Okuda T, Yoshida N, et al. Identification of the novel AML1 fusion partner gene, LAF4, a fusion partner of MLL, in childhood T cell acute lymphoblastic leukemia with t(2;21)(q11;q22) by bubble PCR method for cDNA. Oncogene. 2008;27:2249–56. doi:10.1038/sj.onc.1210857.
38. Mikhail FM, Coignet L, Hatem N, Mourad ZI, Farawela HM, El Kaffash DM, et al. A novel gene, FGA7, is fused to RUNX1/AML1 in a t(4;21)(q28;q22) in a patient with T cell acute lymphoblastic leukemia. Genes Chromosomes Cancer. 2004;39:110–8. doi:10.1002/gcc.10302.
39. Kitamura T. New experimental approaches in retrovirus-mediated expression screening. Int J Hematolv. 1998;67:351–9. doi:10.1016/S0925-5710(98)00025-5.